Sedimentation associated with glaciovolcanism: a review

Smellie, J.L.

School of Geography, Geology and the Environment, University of Leicester LE1 7RH, UK

Email: jls55@le.ac.uk

Abstract

Three discrete categories of sedimentary deposits are associated with glaciovolcanism: englacial cavity, jökulhlaup and lahar. Englacial cavity deposits are found in water-filled chambers in the lee of active glaciovolcanoes or at a locus of enhanced geothermal heat flux. The cavities provide a depocentre for the accumulation of debris, either abundant fresh juvenile debris with sparse dropstones (associated with active glaciovolcanism) or polymict basal glacial debris in which dropstones are abundant (associated with geothermal hot spots). Described examples are uncommon. By contrast, volcanogenic jökulhlaup deposits are abundant, mainly in Iceland, where they form extensive sandar sequences associated with ice-*covered* volcanoes. Jökulhlaups form as a result of the sudden subglacial discharge of stored meltwater. Analogous deposits known as glaciovolcanic sheet-like sequences represent the ultra-proximal lateral equivalents deposited under the ice. Glaciovolcanic lahars are associated with ice-*capped* volcanoes. They form as a result of explosive eruptions through relatively thin ice or following dome collapse, and they trigger mainly supraglacial rather than subglacial meltwater escape. Sediment transport and depositional processes are similar in jökulhaups and lahars and are dominated by debris flow and hyperconcentrated or supercritical flow modes during the main flood stage, although the proportions of the principal lithofacies are different.

Introduction

Glaciovolcanism is defined as '*all types of volcano interactions with ice in all its forms (including snow and firn) and, by implication, any meltwater derived from that ice by volcanic heating*' (Smellie, 2006). It is widespread on Earth, extending from the equator to both polar regions (Major and Newhall, 2989; Smellie and Edwards, 2016; Curtis and Kyle, 2017; Barr et al., 2018; Edwards et al., 2020; Fig. 1). The study of glaciovolcanism is a relatively young science but it is a distinctive and important component of hydrovolcanism (Edwards et al., 2015; Smellie and Edwards, 2016). It has a history of investigations going back only about a century but has undergone an exponential growth in interest during the past few decades (Russell et al., 2014). In part, this is due to the occurrence of two particularly significant well-monitored glaciovolcanic eruptions, both in Iceland: Gjálp in 1996 (Gudmundsson et al., 1997) and Eyjafjallajökull in 2010 (Gudmundsson et al., 2012; Magnússon et al., 2012). The latter eruption, in particular, had a widespread and extremely costly impact on aviation, tourism and business travel for the duration of the eruptive period (Smellie and Edwards, 2016, p. 4). Glaciovolcanic eruptions have the power to reshape the surrounding landscape, often causing massive environmental damage mainly by ashfall, glacier outburst floods (jökulhlaups) and lahars (e.g. Carrivick et al., 2004b; Russell et al., 2006; Huggel et al., 2007 ; Friele et al., 2008; Dunning et al., 2013; Harrison et al., 2019; Thouret et al., 2020; Delgado Granados et al., 2021).

Post-
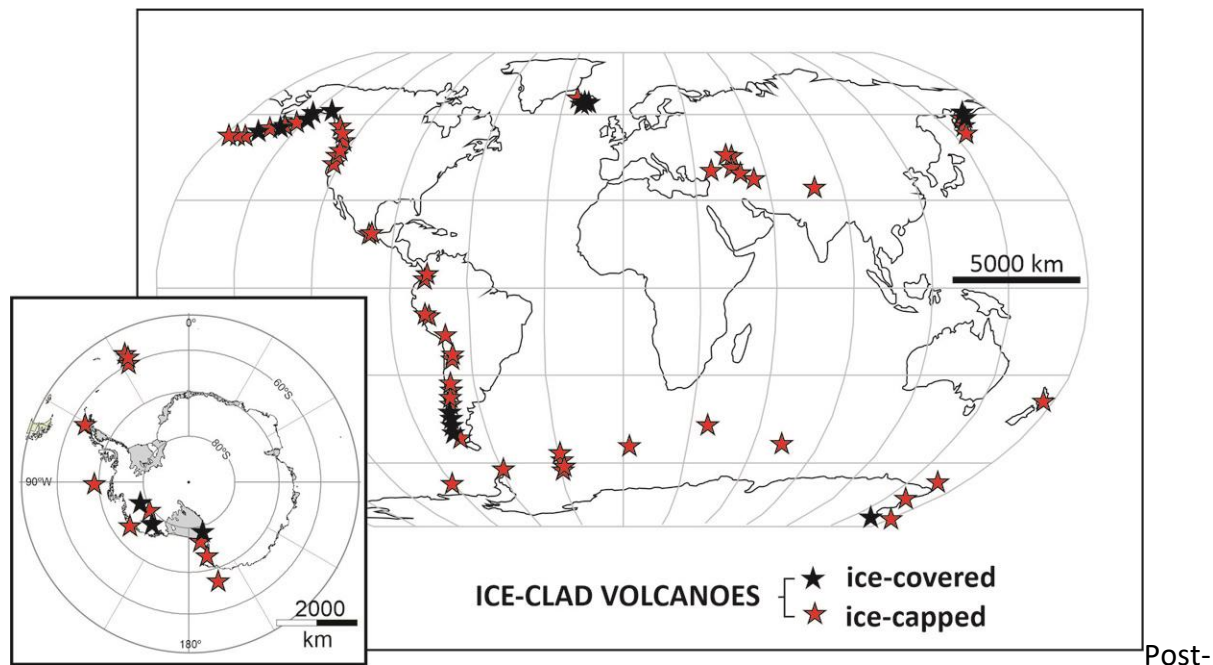
Figure 1.   Map showing the global distribution of Holocene glaciovolcanoes (based on Edwards et al., 2020, modified). The inset shows an expanded view of Antarctica, which is poorly displayed on the main map due to the projection. The volcanoes are divided into ice-capped and ice-covered, as explained in the text and as they occur today. Ice-covered volcanoes are concentrated mainly in polar and sub-polar locations. However, most are ice-capped polygenetic stratovolcanoes associated with circum-Pacific consuming plate margins. During past glacials, the numbers and distribution of ice-covered volcanoes expanded towards lower latitudes, affecting additional volcanoes especially in Alaska and Patagonia, and probably including all of Antarctica's volcanoes.

eruptive erosion is ubiquitous and affects all volcanoes including those erupted in non-glacial settings and the resulting sedimentary products have been well described by many authors, in particular in the seminal volume by Fisher and Smith (1991) and elsewhere in this volume. The wide range of natural post-eruptive erosional processes includes not only erosion by overriding glacial ice but also edifice degradation caused by gravitational collapses during ice-free or ice-poor interglacial periods when the buttressing effect of the surrounding ice is removed. These processes result in significantly modified landforms and a variety of epiclastic sediments, although neither aspects are generally well described (Smellie et al., 1993; Loughlin, 2002; Tuffen et al., 2002; Komatsu et al., 2007a). Because the processes result in normal epiclastic, mainly mass flow deposits that are not linked directly to active glaciovolcanism, they are not discussed further. Thin diamict drapes relating to younger glacial episodes, which have been observed on many glaciovolcanoes (Jones, 1969; Werner and Schmincke, 1999; Loughlin, 2002), are also excluded.

To date, practically all of the emphasis of investigations of glaciovolcanoes by volcanologists has been focused on the ice-clad volcanic edifices and the primary eruptive products, i.e. the lavas and tephras (e.g. Smellie, 2001, 2006, 2008; Kelman et al., 2002; Tuffen et al., 2001, 2002; McGarvie et al., 2007; Stevenson et al., 2006, 2009, 2011; Smellie et al., 2011a, 2018; Conway et al., 2015; Edwards et al., 2015; Cole et al., 2018). Associated sedimentary rocks are only rarely described in those investigations, and seldom in detail (Bergh and Sigvaldason, 1991; Loughlin, 2002; Tuffen et al., 2002; Bennett et al., 2006, 2009). However, a major dramatic impact of glaciovolcanism is the occurrence of jökulhlaups (glacial outburst floods) and lahars, which can have a major impact on the local landscape. The products,

processes and landforms associated with jökulhlaups and lahars have been a focus of numerous studies by sedimentologists (e. g. Jónsson, 1982; Scott, 1988; Hackett and Houghton, 1989; Maizels, 1989, 1993, 1997; Baker et al., 1993; Palmer et al., 1993; Scott et al., 1995; Tómasson , 1996; Donoghue and Neall, 2001; Carrivick et al., 2004a,b, 2007; Alho et al., 2005; Russell et al., 2006, 2010a,b; Duller et al., 2008, 2014; Pierson, 2005; Dunning et al., 2013; Pagneux et al., 2015). However, until now there has been no comprehensive overview of sedimentation linked to active glaciovolcanism, and its causes and characteristics. This is particularly true for distinctive deposits sedimented in proximal locations (i.e. at subglacial locations, close to the volcano source). This contribution sets out to redress that imbalance.

Terminology

In this paper, 'englacial' is used to describe cavities that are surrounded by ice. The usage of englacial and subglacial is confused in glaciovolcanology and both words are used in different publications depending on the authors' preferences (cf. Tuffen et al., 2001, 2002; McGarvie, 2009; Smellie et al., 2011a; Russell et al., 2021). Following glaciological usage, englacial implies that ice should be present on *all* sides. However, since the initiation of glaciovolcanic eruptions is typically at a bedrock surface overlain by ice, 'subglacial' is often preferred. Etymologically, the prefix 'en' is used in English to signify 'to put someone or some thing into or onto', with no assumption of being *completely* surrounded. Moreover,
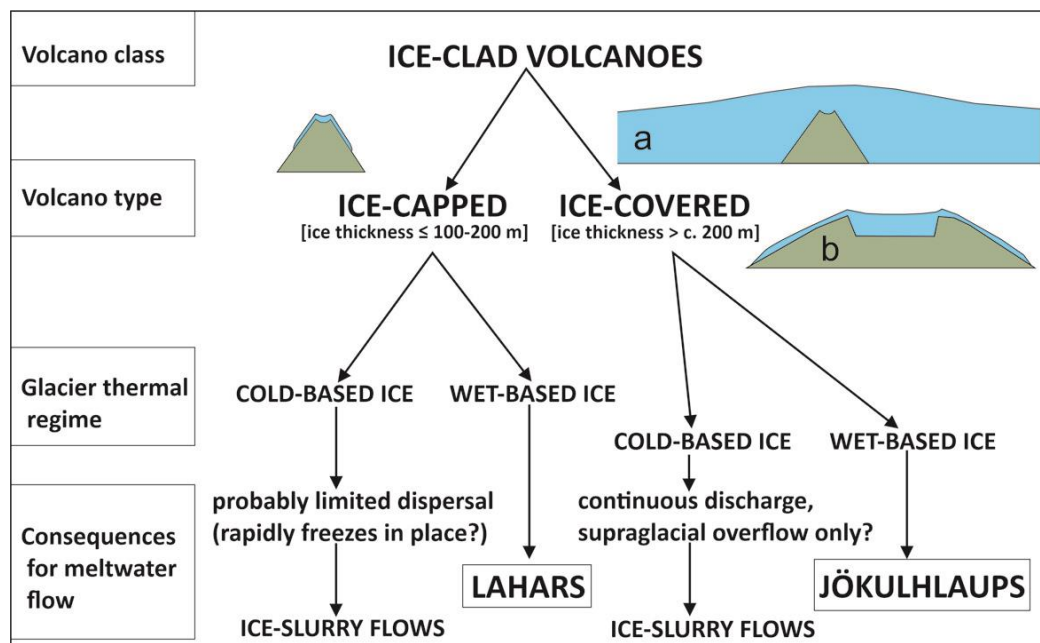
Figure 2. Classification of ice-clad volcanoes, as used in this paper. Ice-covered volcanoes are distinguished by ice thicknesses > c. 200 m *over the vent*. Hence, in addition to volcanoes that are drowned by an ice sheet (labelled a), they also include edifices that have summit calderas filled by thick ice but have thinner ice (often < 200 m) on the flanks (labelled b). 'Ice' includes any snow and firn present. The consequences for meltwater discharge and resulting deposits are also shown for different glacier thermal regimes. In both ice-capped and ice-covered settings, it is likely that eruptions under cold-based ice result only in highly mobile meltwater flows or ice-slurry flows (e.g. Lube et al., 2009) with a negligible potential for preservation or recognition. Not to scale. See text for further details.

many glaciovolcanoes grow upwards and ultimately penetrate the surface of the overlying ice. Thus an eruption that commences subglacially evolves to become subaerial, whilst still confined by ice on its flanks. It is then neither englacial nor subglacial but simply ice-

impounded, potentially leading to a plethora of names required to describe a single edifice. In this paper, the term 'englacial' is used simply to imply that a cavity associated with glaciovolcanic activity (including geothermal activity lacking an associated volcanic eruption) is surrounded by ice on most of its sides.

Volcanoes with an ice cover (including any snow and firn) are here called **ice-clad**. A further distinction is made between ice-capped and ice-covered (Figs 2, 3). It follows from the division proposed by Smellie and Skilling (1994) and Chapman et al., (2000) in which a
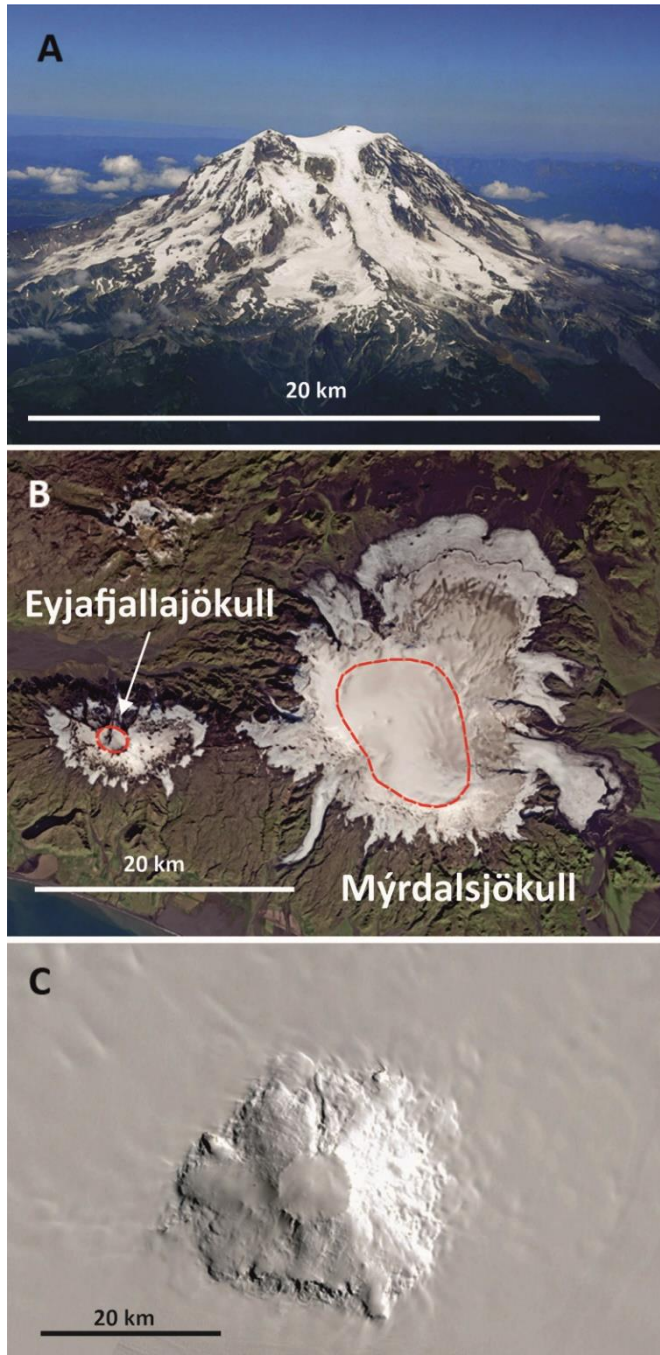
Figure 3. Views of selected ice-clad volcanoes. A. Mount Rainier, USA, an active ice-capped volcano with a summit elevation of c. 4000 m. Photo by Stan Shebs (https://en.wikipedia.org/wiki/GNU_Free_Documentation_License). B. Satellite image showing Mýrdalsjökull (Katla volcano) and Eyjafjallajökull, southern Iceland. Caldera outlines are indicated by red dashed lines. Both are active ice-covered volcanoes but the thickness of ice within the summit caldera of Eyjafjallajökull (c. 200 m)

is at the transition separating ice-capped and ice-covered volcanoes, and the lateral extent of the ice on the volcano is quite limited. Eruptions in the Eyjafjallajökull caldera (e.g. that in 2010) create a meltwater-filled englacial vault that is short-lived and drains as a jökulhaup soon after an eruption starts (see Magnússon et al., 2012, for the sequence of events in 2010). Should the capping ice become thinner in future, the volcano shall be classified as ice-capped. Ice within the Katla caldera is 400-700 m thick (Björnsson et al., 2000) and meltwater stored initially during eruptions is eventually released subglacially via glaciers that breach the caldera (e.g. Tómasson, 1996). NASA Earth Observatory image by Jesse Allen, using Landsat data from the U.S. Geological Survey. C. Satellite view of Mount Takahe, an active ice-covered volcano in Antarctica. The thickness of ice within the prominent summit caldera is unknown but likely to exceed 200 m. However, unlike ice-covered volcanoes in Iceland, the implications for meltwater escape (and therefore jökulhlaups) are uncertain. Although high thermal gradients within the caldera caused by the cooling magma chamber might create local areas of wet-based ice, much of the volcano is covered by cold-based ice, and basal meltwater escape will be difficult. Image: Google Earth and U.S. Geological Survey.

distinction was drawn between thin- and thick-ice conditions. Under thin ice, i.e. ≤ 100-200 m (Smellie and Skilling, 1994; Chapman et al., 2000; see also Edwards et al., 2015; Curtis and Kyle, 2017), also called mountain ice or alpine ice, the glacial topography forms an icefield and the underlying topography of the volcano is clearly evident and exerts a powerful control on ice flow. The glacial cover offers little impediment to explosive eruptions and meltwater probably escapes continuously. These volcanoes are here called **ice-capped** in recognition that the glacial cover is a geographically limited capping mass and the lower slopes of the volcanoes are generally ice-free except for far-travelled glaciers (Fig. 3a). By contrast, **ice-covered** volcanoes are those which are draped by a geographically extensive sheet of ice, which covers much or all of the volcano and may extend far beyond the morphological limits of the volcano (Figs 2b,c). On these edifices, the thickness of ice *above the vent* is more than c. 200 m. For eruptions beneath ice > 200 m thick, explosivity is largely suppressed initially and a water filled vault is created. In general, ice-covered volcanoes are characteristic of the polar and sub-polar regions whereas ice-capped volcanoes are overwhelmingly dominant at mid and lower latitudes (Fig. 1). However, the discrimination between the two types of volcano is not rigorous and many volcanoes have summit calderas in which the ice exceeds 200 m in thickness whereas ice thicknesses on the flanks are just tens of metres (e.g. Mýrdalsjökull and Öræfajökull in Iceland; Hudson volcano in Chile; Naranjo and Stern, 1998; Björnsson et al., 2000; Magnússon et al., 2013; Fig. 4). On these
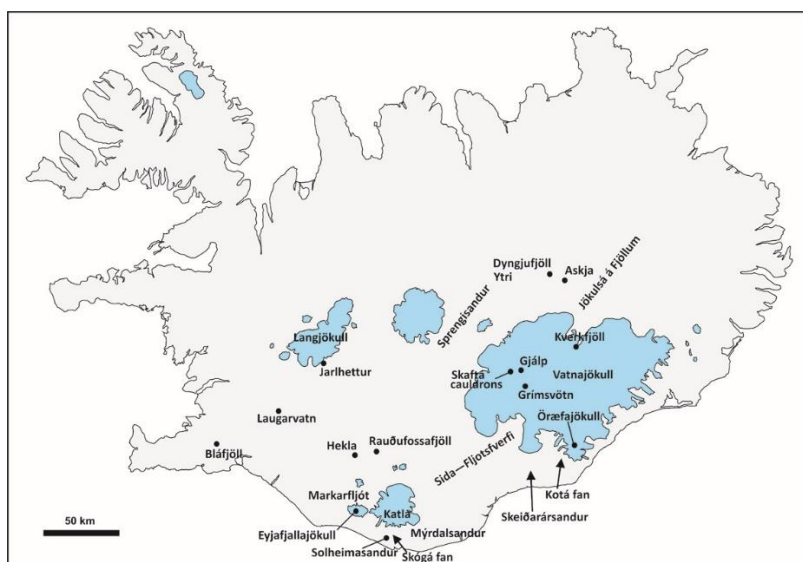
Figure 4. Map of Iceland showing the locations of places mentioned in the text.

volcanoes, the style of eruptions from summit vents will be different from those occurring at flank vents, with significantly different implications for the timing and volumes of meltwater and associated sediments. Further distinction can be made according to the glacial thermal regime (Fig. 2), which will determine the hydraulics of the volcanic eruption (as described below), the shape of the hydrograph of any meltwater discharge and the sedimentation paths.

Deposits that are linked to erupting subaqueous (including subglacial) volcanoes are characteristically dominated by juvenile clasts that may be redeposited more or less contemporaneously while in an unlithified state (i.e. the syn-eruption resedimented deposits of McPhie et al., 1993). As a result, the deposits are highly immature and closely resemble primary volcaniclastic rocks both texturally and compositionally. Many volcanologists therefore use primary volcaniclastic names for rapidly resedimented deposits, formed dominantly of juvenile clasts (White and Houghton, 2006). Conversely, epiclastic terminology is used for deposits, usually polymict, showing evidence for erosion of previously lithified bedrock or whose particles differ in size and shape , especially evidence for abrasion during transport, from those formed during an eruption. However, a significant problem exists when discussing some clastic rocks associated with glaciovolcanism. As is described later, proglacial deposits of eruption-related jökulhlaups (glacier outburst floods) have been universally described by sedimentologists using epiclastic terminology. By contrast, the more-proximal subglacial equivalents of jökulhlaup deposits, known as glaciovolcanic sheet-like sequences (Smellie, 2008), have been described by volcanologists using volcaniclastic terminology. Thus, different parts of essentially the same deposits are currently described using contrasting terminology simply because of the location in which they were finally deposited (subaerial versus subglacial). In part this is because turbulent flow conditions associated with jökulhlaups (and lahars) are capable of eroding and incorporating additional debris from the surface over which they pass. Thus, whilst often dominated by juvenile volcanic clasts generated by the coeval eruption, the flows can become polymict due to a process called bulking up (described later). Moreover, clasts often show abrasion (rounding) mainly due to erosion of fluvial sediments from the substrate, although if the substrate becomes scoured of easily erodable detritus, angular juvenile detritus may become dominant in younger flows. In this contribution, to enable the easiest comparison with published studies, the terminology used in the original publications is used except where it is unambiguously incorrect (e.g. use of epiclastic terminology for deposits when they are clearly primary volcanic lithofacies that constructed volcanic edifices (i.e. monomict, angular-clast tephras and volcanic breccias; see Bennett et al., 2009). Additionally, most published studies of Icelandic volcanic outcrops conflate lapilli tuff, pillow breccia and hyaloclastite. They are typically all referred to as hyaloclastite despite the significant differences in the generation of those deposits. In this contribution, the terminology of White and Houghton (2006) is used for those volcanic lithofacies following the recommendations of Smellie and Edwards (2016).

Hydraulics of glaciovolcanic eruptions

The hydraulics of fluid flow in glaciers is of fundamental importance for understanding the timing, volume and transport paths of sediment moved during glaciovolcanic eruptions. The different thermal states of glaciers have profound differences for meltwater hydraulics. Glaciers and ice sheets occur in two broad end-member thermal regimes: cold-based ice (also called polar or frozen-bed ice) in which all the ice is below the pressure melting point

and the ice is frozen to its bed, and warm-based ice (also called wet-based or temperate ice) in which the ice is at or close to the pressure melting point throughout. An intermediate thermal state, called polythermal or sub-polar ice, comprises ice with a thin basal layer at the pressure melting point, or a patchwork mosaic composed of cold- and warm-based ice; in the former, a thin layer of meltwater intervenes between the ice and bedrock similar to warm-based ice whilst, in the latter, the individual patches have the same properties as cold- or warm-based ice. Although there are some practical differences between polythermal ice and both cold- and warm-based ice, they are relatively minor and for present purposes polythermal ice does not require a separate discussion.

The treatment followed here is focused principally on eruptions associated with warm-based ice, which is the overwhelmingly dominant thermal regime of ice on Earth (but not on other planets, e.g. Mars: Carr and Head, 2010; Hubbard et al., 2014) and in which sub- and englacial meltwater is a defining feature. The overlying ice is decoupled from its bedrock, thus permitting the ice to slide. Wet-based ice is thus much more dynamic than cold-based ice, which moves principally by slow internal deformation. Moreover, since meltwater generated during a volcanic eruption under cold-based ice conditions is sealed into an encircling vault by the enclosing ice, the ice cannot be floated and the meltwater can only escape supraglacially. This has implications for the constituent sedimentary materials and volumes of sediment transported, as will be discussed later.

Water is transmitted only very slowly by Darcy flow along ice crystal boundaries in snow and firn and effectively not at all in ice, apart from in microfractures and crevasses. However, snow and firn particles readily melt and cause the bulk porosity and permeability to constantly change (Fig. 5). This is particularly true during the seepage of warm, volcanically
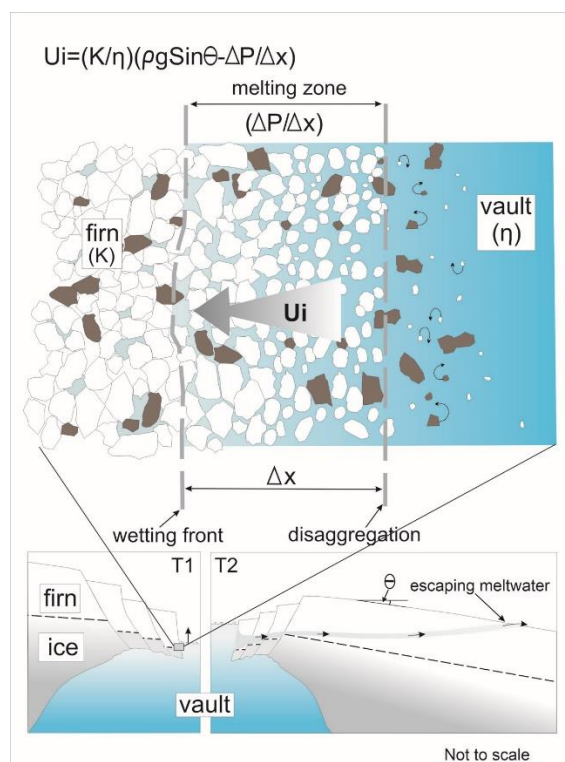
Figure 5. Schematic diagram illustrating the melting processes and migration of meltwater through firn or snow at the margins of a warm, meltwater-filled vault during a glaciovolcanic eruption (adapted from Smellie, 2006). The ice particles melt continuously as the wetting front moves forward, altering the porosity and considerably increasing the relative permeability. Meltwater penetration is thus enhanced leading to

supraglacial escape. The grey objects are rock particles. Abbreviations: T1 – vault at time 1 (vault filling); T2 – vault at time 2 (vault overflowing); u_i – water volume flux per unit area; K – intrinsic (hydraulic) permeability of the aquifer medium (firn/snow); ΔP/Δx – pressure or hydraulic gradient; η – dynamic viscosity of water. See Smellie (2006) for further discussion.

heated meltwater and it can lead to supraglacial drainage (overflowing), ultimately by pipe flow in tunnels during glaciovolcanic eruptions (Smellie, 2006). In warm-based ice, meltwater moves along the ice:bedrock interface either as slow distributed flow or faster channelized flow (Björnsson, 1998; Fountain and Walder, 1998). The latter is faster because it occurs within Nye and Röthlisberger channels, also called N and R channels, eroded in bedrock and ice, respectively. Their presence is of fundamental importance for understanding why englacial vaults created during volcanic eruptions are essentially leaky, when they are developed above pre-existing subglacial channel networks (Smellie, 2006, 2018). Even if the eruptive site and associated englacial vault do not intersect a pre-existing tunnel network, Glen's Law predicts that, at ice thicknesses exceeding 150-200 m, the horizontal stress at the ice:bedrock interface exceeds the vertical compressive stress thus theoretically enabling water in the vault to force a hole in the ice and potentially link up with any tunnels in the vicinity (Glen, 1954; but see Tweed and Russell, 1999). The development and relative proportions of supraglacial and subglacial drainage are important for understanding flood timing, sediment transport paths and meltwater volumes.

It is also important to recognize that abundant meltwater can be produced in areas of high geothermal heat flow even without volcanic eruptions. These lead to distinctive ice surface features known as cauldrons caused by the collapse of the underlying ice (less dense than water). They are often associated with jökulhlaups, for example the Skaftá cauldrons in Iceland (Fig. 6; Einarsson et al., 2017). The very long cooling times for crustal magma

Figure 6. View of one of the Skaftá cauldrons (Vatnajökull, Iceland), which are caused by geothermal heat melting the overlying ice, causing the surface to subside. The feature is c. 2 km in diameter. Photograph by the author. All photographs in this paper are by the author unless otherwise attributed.

chambers associated with large polygenetic glaciovolcanoes may cause enhanced geothermal heat that can persist for many thousands of years, creating large water-filled englacial vaults that may be emptied repeatedly in jökulhlaups (e.g. Björnsson, 1988, 1992; Gudmundsson et al., 2007; Russell et al., 2010a; Einarsson et al., 2017).

Glaciovolcanic edifices and effect on timing and volumes of meltwater generation

For ice-capped volcanic edifices, the hydraulic consequences of eruptions are relatively simple. The cover of relatively thin ice (which includes snow and firn) is unable to suppress explosive eruptions, resulting in the construction of prominent pyroclastic cones (e.g. Smellie, 2002; Magnússon et al., 2012). Nor does the thin ice significantly impede the flow of meltwater, which escapes generally within minutes, or at most a few hours, of an eruption initiating (e.g. Kjartansson, 1951; Waitt et al., 1983; Scott, 1988; Pierson et al., 1990; Trabant et al., 1994; Pierson, 1995; Magnússon et al., 2012). By contrast, the volcanic and hydraulic consequences for edifices that are ice-covered (i.e. ice > 200 m thick over the vent) are significantly different. Two broad types associated with thick ice can be distinguished based on the dominant constructive process. The first type mainly comprises tephra-bearing edifices in which explosive hydrovolcanism is prominent, resulting in glaciovolcanic tuff cones or tindars which are constructed in a meltwater-filled englacial vault. A tindar is a volcanic ridge constructed by a subglacially erupted, overlapping series of tuff cones along a volcanic fissure (Jones, 1969, 1970); it is often surmounted by laterally spreading lava-fed deltas if the edifice becomes subaerial, when it is called a tuya. Glaciovolcanic sheet-like sequences (sensu Smellie, 2008) can also form in these situations; although the type of edifice responsible for sheet-like sequences has not yet been described, it is probably a glaciovolcanic tuff cone or tinder (Smellie and Edwards, 2016). A second type of edifice formed under thick ice conditions forms non-explosively and is dominated by subaqueous lava effusion (pillow mounds, glaciovolcanic domes and lava-dominated tuyas; Jones, 1969; Smellie and Edwards, 2016). It may transition up into explosive hydrovolcanic activity, as just described, but many examples cease at the effusive subglacial stage (e.g. McGarvie et al., 2007; Pollock et al., 2014). Absence of explosivity indicates that substantial pressure over the erupting vent exists typically corresponding to an ice roof thickness or meltwater depths ≥ 100-200 m (Jones, 1969; White et al., 2003; Zimanowski and Buttner, 2003). The hydraulic conditions are broadly similar in each case, involving initial meltwater build-up in an englacial vault encompassing the active volcanic edifice, during which time the meltwater leaks more or less continuously at the ice:bedrock interface, as exemplified by the well-documented glaciovolcanic eruption of Gjálp (Iceland) in 1996 (Fig. 7; Gudmundsson et al., 1997). Eventually floating of the surrounding ice occurs
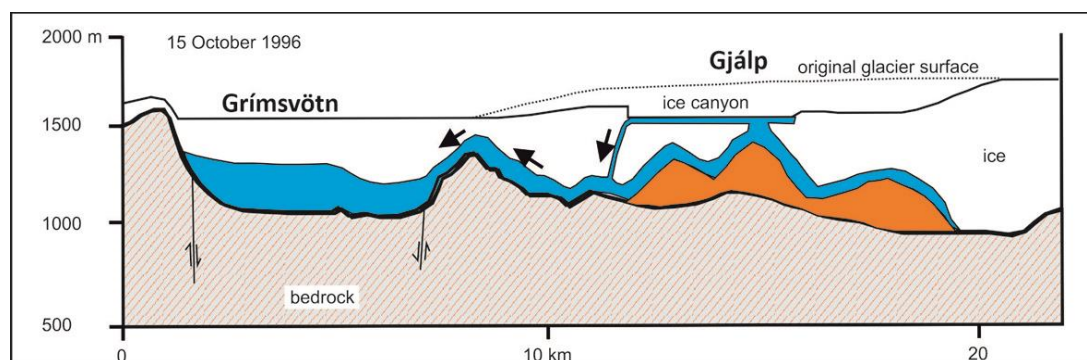
Figure 7. Schematic cross section showing features of the 1996 eruption of Gjálp, Iceland (after Gudmundsson et al., 1997). Note the evidence for both subglacial and supraglacial meltwater drainage (black arrows). The

9

meltwater generated at Gjálp was temporarily stored in the Grímsvötn caldera before being released in a major jökulhlaup on Skeiðarársandur. Thus, the debris carried in the jökulhlaup was derived largely from the Grímsvötn basin and eroded from the subglacial transport path between there and the terminus of Skeiðarárjökull. It does not directly reflect the nature of the glaciovolcanic eruption at Gjálp.

if the hydraulic pressure at the base of the water-filled vault balances the encircling cryostatic pressure, thus initiating a sudden outburst flood (jökulhlaup). Compared to eruptions at ice-capped volcanoes, there will be a strong delay in timing before the initiation of any jökulhlaup, amounting to several days or even weeks depending on the local conditions, especially thickness of ice being melted (Tómasson, 1996; Gudmundsson et al., 1997). A principal difference between the two eruption modes at ice-covered volcanoes is in the rapidity of meltwater generation. It is much more efficient and thus faster during type 1 hydrovolcanic explosivity than during type 2 passive lava effusion (Gudmundsson, 2003). However, passive lava effusion *by itself* will not result in floating of the surrounding ice. The slow conductive melting of the ice may only keep pace with the essentially continuous basal escape of meltwater, and conditions in the vault are never likely to be sufficient to break the ice seal by flotation. Thus, no jökulhlaup is likely to occur. The resulting hydrograph may broadly resemble that associated with eruptions under alpine ice although the slow generation of meltwater may significantly reduce the peak discharge.

During jökulhlaup events, the escaping meltwater follows multiple routes through a glacier or ice sheet. Basal flow is mainly in tunnels rapidly enlarged by heat transferred from the volcanically-heated meltwater and by viscous dissipation. The sudden injection of water during some jökulhlaups can overwhelm the tunnel system leading to a distributed, linked-cavity system, decoupling of the glacier from its bed, and a glacier surge (Björnsson, 1998). Supraglacial flow can also occur either by overflowing of the englacial lake or as a result of pressurized water forcing a way up crevasses (e.g. Gudmundsson et al., 1997; Roberts et al., 2000; Waller et al., 2001; Smellie, 2002, 2006; Russell et al., 2010a,b; Figs 7, 8); supraglacial overflow is in any case the only way in which meltwater can escape during eruptions under cold-based ice. For subglacial discharge, the glacier snout is frequently disintegrated by the forceful exit of over-pressured meltwater, resulting in the generation of numerous ice blocks often tens of metres across that are diagnostic of jökulhlaups (Fig. 8). Sediment can be transported along any of these escape routes.
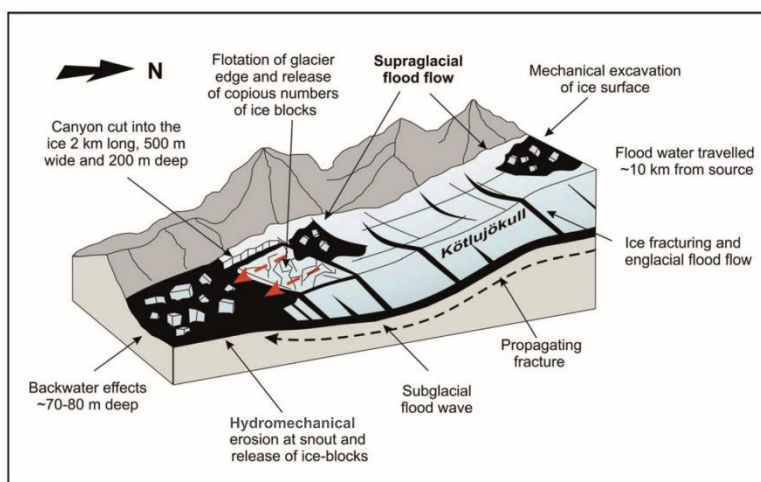
Figure 8. Cartoon showing hydraulics of meltwater flow at the snout of a glacier during a jökulhlaup (from Russell et al., 2010a, fig. 11.5). Note how the over-pressured water has forced its way up crevasses as well as

exiting at the snout via tunnel portals. Glacier snouts frequently break up en masse, contributing large numbers of often very large icebergs to the jökulhlaup.

Three categories of sedimentary deposits associated with glaciovolcanic eruptions

The major focus of this contribution is on deposits associated with glaciovolcanic eruptions and during periods of enhanced subglacial geothermal heat flow, often very long-lived, that do not result in a volcanic eruption. Moreover, an important consequence of the distinction into ice-covered and ice-capped volcanoes (Fig. 2) is that eruptions beneath thick ice, as defined above (i.e. ice-covered), characteristically yield **jökulhlaups** (sudden large-volume floods of meltwater released by ice-confined lakes after a period of impoundment) and their deposits. By contrast, eruptions under thinner alpine ice at ice-capped volcanoes are unable to pond significant volumes of meltwater and its discharge is essentially continuous from the earliest stages of an eruption. The latter result in flows known as **lahars** together with their deposits. Although the products of jökulhlaups and lahars are similar (combinations of debris flow and hyperconcentrated flow deposits), their triggering conditions (i.e. lake flood versus snowmelt/ice scour) are different and they are generally treated as distinct types of mass flows (e.g. Gudmundsson, 2015; Curtis and Kyle, 2017; Barr et al., 2018). The hydrographs are also similar, with a steep rising stage and much more gradual falling stage. Although lahar hydrographs are perhaps more often multi-peaked during the falling stage, there is no clear distinction with jökulhlaups (cf. Maizels, 1997; Pierson et al., 1990; Pierson, 1995; Lube et al., 2009). Three major categories of clastic deposit types associated with glaciovolcanism can be distinguished based on differences in structural setting (a combination of geothermally active sites with or without volcanic activity; and volcanic eruptions beneath thick and thin ice). They comprise (1) englacial cavity deposits; (2) jökulhlaup deposits; and (3) lahar deposits.

Englacial cavity deposits

In present context, englacial cavities are voids created by melting due to geothermal heat associated with glaciovolcanism. Typically, they form above a glaciovolcanic edifice during an eruption but they are also created above areas of long-lived high heat flow associated with large polygenetic volcanoes and the prolonged cooling of their magma chambers (Gudmundsson et al., 2007; Einarsson et al., 2017). Only static ice conditions have previously been considered (and are usually unstated) in models for erupting glaciovolcanoes but, given that most bedrock surfaces are not horizontal but have gradients, glaciovolcanism associated with moving ice must occur frequently in nature. Away from steep gradients, ice movement is typically very slow in most ice masses (few metres to tens of metres yr^{-1}; Hambrey and Glasser, 2005) so an assumption of effectively static ice is realistic for short-lived eruptions (months to few years). However, much faster flow occurs in ice streams and outlet glaciers, and on steep gradients (few kilometres yr^{-1}; Rignot et al., 2011). Only a single model has been published for a glaciovolcanic centre that is postulated to have erupted under fast-moving ice (an ice stream), which resulted in a distinctive constructive architecture and volcanic lithofacies (Smellie and Panter, 2021). Most glaciovolcanoes described so far are small monogenetic centres for which the build-up, release & decay of geothermal heat occur over short timescales (weeks, months or, at most, a few years). Thus, the assumption of essentially static ice is permissible in most instances even when that ice is in reality moving slowly. However, for larger polygenetic centres or monogenetic centres associated with long-lived volcanic fissure systems, the lifetime of above-background geothermal heat is considerably extended (for example, a decay lifetime of c. 50 ka is not

unusual for high-level crustal magma chambers associated with large polygenetic centres; Fassett and Head, 2006, 2007). If ice moves rapidly across a geothermal hot spot, an asymmetrical englacial cavity is created on the lee side. For the cavity to be filled with meltwater, relatively thick ice (> 100-200 m) is required. Such a situation has been described in detail for two examples associated with volcanic fissures in Iceland by Bennett et al. (2006, 2009) and they are summarized here.

Subglacial glaciolacustrine fans have been identified in Iceland associated with prominent volcanic fissure systems in the Laugarvatn and Brekknafjöll—Jarlhettur areas (Fig. 9). Similar deposits have not been described by other authors elsewhere, which implies that the
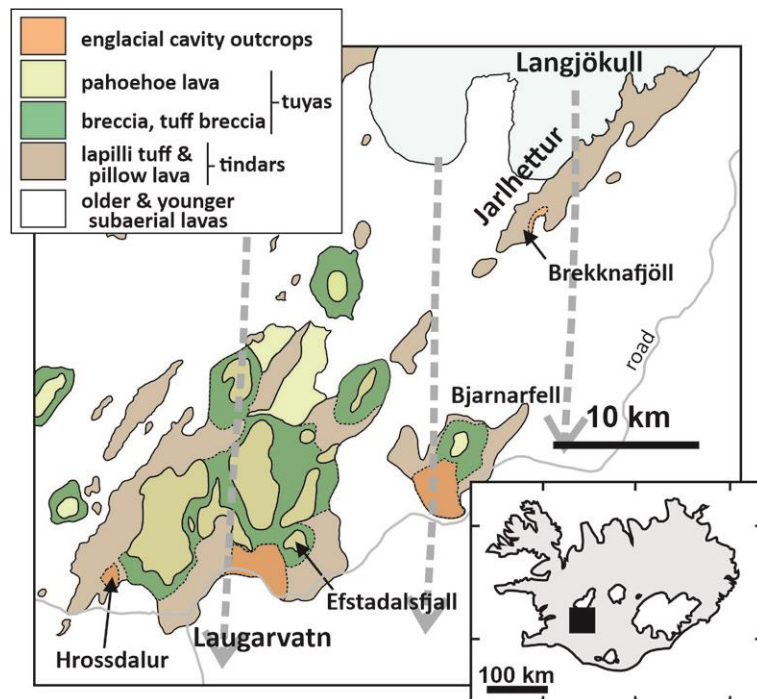
Figure 9. Simplified geological map of the area between Laugarvatn and Brekknafjöll—Jarlhettur (modified after the Geological Survey of Iceland (http://jardfraedikort.is/?coordinate=64.23%2C-20.45&zoom=3) and Jones, 1969), showing the locations of known outcrops of englacial cavity (glaciolacustrine) deposits (after Bennett et al., 2006, 2009). The glaciolacustrine outcrop in the Jahrlhettur area is approximate and others may exist there. The outcrops of breccia/tuff breccia of the lava-fed deltas (tuya edifices) are estimated. Palaeo-ice sheet flow lines (grey arrows) after Hubbard et al. (2006). The inset shows the location of the map within Iceland.

deposits might require unusual conditions for their formation and preservation. In the **Laugarvatn area**, glaciovolcanism is represented by multiple overlapping tindars and tuyas that erupted at different times during the Quaternary (< 780 ka) from a prominent north-east-trending fissure system. The centres are historically significant in that they were a focus of one of the earliest glaciovolcanic studies, in which a general model for glaciovolcano construction was established (Jones, 1969, 1970). Two sedimentary fan successions were described by Bennett et al. (2006). One, at Efstadalsfjall (Fig. 9), is c. 1.5 km in length (apex to toe) and up to 3.5 km in width, formed of deposits that vary from 25-35 m thick in distal parts to < 10 m near the fan apex. The sedimentary dips decline in a south-westerly direction progressively from 24-28° in the main part of the fan to < 5° distally. The second fan, at Hrossdalur (Fig. 9) is smaller and less well exposed, measuring c. 1.2 km long and up to 800 m wide, composed of sedimentary deposits that attain a maximum thickness of 33-55 m. The fans, and a third fan at Bjarnarfell nearby (otherwise undescribed), are confined

to the down-flow (lee) side of the volcanic edifices relative to the prevailing ice flow direction, but they drape the edifices to a high elevation. They are constructed from successive sedimentary sheets orientated sub-parallel to the fan surface, which onlap volcanic rocks composed mainly of pillow lava and pillow breccia representing basal pillow mounds and overlying breccia/tuff breccia foreset bedded deposits of tuyas (Jones, 1969, 1970). The beds are cross-cut by numerous large (> 50 m) and small (< 30 m) channels, which are broader distally. The deposits are polymict and contain little or no primary (juvenile) volcanic material. They are dominated by abraded (sub-rounded—sub-angular) volcanic clasts, and many clasts show striations and facetting. Six recurrent epiclastic facies assemblages were defined including massive to stratified diamicts, in which dropstones are common; gravel, sand and silt sheets and channel fills; and laminated silts and rhythmites, also with numerous dropstones (Figs 10, 11). Although the deposits are essentially lithified (i.e. diamictite, conglomerate/breccio-conglomerate, sandstone, siltstone etc), the

Figure 10. Selected sedimentary logs of glaciolacustrine sequences at (A) Eftadalsfjall and (B) Brekknafjöll (from Bennett et al., 2006, 2009). In B, note the presence of juvenile debris in the clast population at Brekknafjöll (inset), significantly more angular than associated polymict debris and consistent with coeval active glaciovolcanism. See Bennett et al. (2006) for explanation of the lithofacies notations.

terminology used by Bennett et al (2006) is that for unlithified deposits. It is retained here to facilitate direct comparison with their study. After advancing arguments rejecting the possibility that the sediments might be related to marine sedimentation during a high sea-level period or deposition in an ice-dammed lake, Bennett et al. (2006) postulated the

existence of a subglacial cavity and sediment depocentre on the lee (southern) side of the Laugarvatn volcanic edifices. The local presence of subglacial diamicts overlying the Hrossdalur fan is also consistent with an ice-confined setting. The sediments were

Figure 11. Selected close views of polymict glaciolacustrine lithofacies characteristic of englacial cavity deposits at Eftadalsfjall (from Bennett et al., 2006). A. Laminated siltstone and mudstone interbedded with thin clast-supported diamicts showing evidence for current winnowing. B. Laminated diamict with siltstone stringers and dropstones passing up into massive to weakly stratified diamict. C. Prominent abraded dropstone in laminated siltstone and mudstone. D. Laminated diamict, a common lithofacies, with small scour structures, silty drapes and numerous small dropstones. E. Abundant abraded dropstones within laminated diamict.

interpreted as products of subaqueous rain-out of subglacial debris associated with rapid suspension settling and some current reworking (represented by massive and stratified diamicts); deposition from fast-flowing, often substrate-eroding sediment gravity flows, variably hyperconcentrated and concentrated flows and turbidity currents (gravel, sand and silt sheets and channel fills); and rapid suspension settling or fine-grained turbidity currents in a quiet-water setting (laminated silts and rhythmites). The presence of abundant dropstones and gravel pods (likely till lumps; cf. Smellie et al., 2011b) in several lithofacies indicate frequent subglacial debris rain-out throughout the sedimentation period.

The creation of an englacial cavity was ascribed to a local high heat flux associated either with the cooling volcanic pile in the immediate post-eruptive period or else a renewed episode of enhanced heat flow. The geothermal heat melted the basal ice as it passed over the volcanic rocks, creating large volumes of meltwater and causing an increased flux of ice-

transported basal polymict debris, which draped the volcanic substrate and created a sediment fan. Although the lithologies comprising the debris were not described by Bennett et al. (2006), it is likely that they were composed almost exclusively of material eroded from the adjacent volcanic centres rather than derived from significantly more distant sources (e.g. beneath Langjökull; Fig. 9). The abraded shapes indicate that the clasts were eroded by the ice and were not redeposited syn-eruptively, suggesting that they were probably not associated with a coeval eruption but with a later episode of geothermal heating. The presence of dropstones throughout also suggests that an ice roof covered the cavity during the depositional period, providing an abundant source of continuously-replenished basal debris (cf. Bennett et al., 2006, fig. 11a). It was suggested that the dimensions of the englacial cavity may have varied with time as a function ice overburden pressure, ice velocity and water volume. The presence of numerous large and small channels suggested the presence of strong currents passing through the vault.

The **Brekknafjöll—Jarlhettur area** consists of several north-east-trending fissures marked by prominent linear ridges (tindars; Fig. 9). It is a north-easterly prolongation of the fissure-erupted volcanic system exposed in the Laugarvatn area but lacks the well-developed tuyas (flat-topped lava-fed delta caprocks) of the latter; tuya development is only incipient. The ridges are characterized by a beaded or serrated appearance due to multiple peaks that represent the sites of individual explosive hydrovolcanic vents that constructed the tindars (Bennett et al., 2009; Smellie and Edwards, 2016, fig. 10.8), many of which were probably simultaneously eruptive. In their study Bennett et al. (2009) described six recurrent lithofacies assemblages. From the published details, use of epiclastic terminology throughout (including for volcanic lithofacies of the tindars) and lack of a geological map, it is difficult to define the full outcrop extent of the epiclastic deposits but they appear to be restricted to a relatively small area on the south-east flank of one of the tindar ridges (Brekknafjöll; Fig. 9); it is likely that additional outcrops exist in the Jarlhettur area. Most of the lithofacies assemblages identified are primary glaciovolcanic (eruptive) deposits and they refer to the construction of the volcanic centres. Only one lithofacies assemblage is epiclastic and is of particular interest (Assemblage 1 of Bennett et al., 2009). It is formed of interbedded massive diamict, stratified diamict and sandy gravels, with lesser laminated silts and laminated diamict (Fig. 12). Because the deposits are lithified they should properly be called diamictite, conglomerate, etc similar to that used for analogous Laugarvatn outcrops,
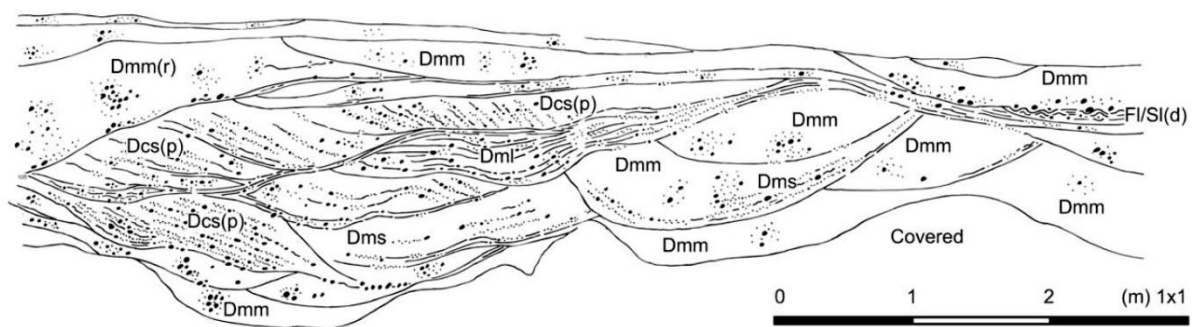
Figure 12. Sketch view of channel-based massive and crudely stratified diamicts in englacial cavity deposits at Brekknafjöll (from Bennett et al., 2009).

but the original terminology is retained here. Larger clasts are sub-rounded to sub-angular, mainly composed of polymict basalts showing abrasion, including striated and facetted

surfaces. They dominate the basal beds, in which dropstones are also locally common. However, angular juvenile clasts are also present. They are generally scarce to absent in basal exposures but their proportion rapidly increases upward and they become dominant. The lithofacies generally rest on sheared diamict that overlies a striated surface cut in subaerial lava. The sedimentary lithofacies form a prominent discordant drape on the glaciovolcanic tindar edifice, whilst at the base of the tindar they are overlain along steep contacts by tindar lithofacies (i.e. mainly pillow lava and lapilli tuff; cf. Skilling, 1994; Smellie, 2001; Schopka et al., 2006; Bennett et al., 2009). The contradicting field relations can be explained by the contemporaneous deformation that the sedimentary deposits have undergone during coeval eruption of the associated tindar (see below). Finer-grained interbedded units display numerous small current scours and the diamicts commonly contain channels up to 0.6 m deep and 8 m in width filled by massive and stratified diamict, some of the latter resembling planar cross sets (Fig. 12). Dropstones are locally common.

The sediments at Brekknafjöll—Jarlhettur are similar in many respects to the fan deposits in the Laugarvatn area. They were interpreted as glaciolacustrine deposits associated with debris rain-out, current reworking and erosional scouring. They form broad low-angled fan accumulations composed mainly of stratified diamicts and matrix- and clast-supported gravel sheets deposited from debris flows, hyperconcentrated flows, and rare turbidity flows respectively. As at Laugarvatn, the occurrence of numerous channels attests to strong water flow and associated diamict remobilization. Quiet water deposits (laminated diamict, silts and rhythmites) are minor and restricted to distal locations. The sites for the latter deposits are sometimes as much as 750 m from the steep ridge margins, attesting to a relatively extensive englacial cavity that in places was wider than the main volcanic ridge itself (typically 400-500 m in diameter).
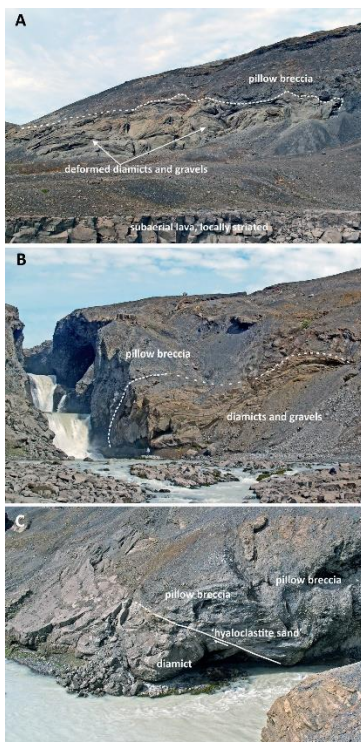
Figure 13. Views of deformed glaciolacustrine englacial cavity deposits on the south-east flank of Brekknafjöll, at Leynifoss. A. View of pale-coloured slumped diamicts and gravels south-west of Leynifoss on the flank of the Brekknafjöll tindar. B, C. Deformed, overturned diamict and gravels, shouldered aside by pillow breccia and

'hyaloclastite sand' (probably lapilli tuff) of the Brekknafjöll tindar. Each of these views is sketched and described by Bennett et al. (2009, figs 17b,c,d, 18).

The field relations between sediments and volcanic rocks at Brekknafjöll—Jarlhettur, and the spectacular large-scale deformation structures shown by the sediments (Fig. 13), were explained by Bennett et al. (2009) as a consequence of the lateral growth of the volcanic core during eruption. The edifice was thus envisaged subsiding into and 'bulldozing' aside the fan deposits while they were still water saturated, soft and easily deformed (Fig. 14).
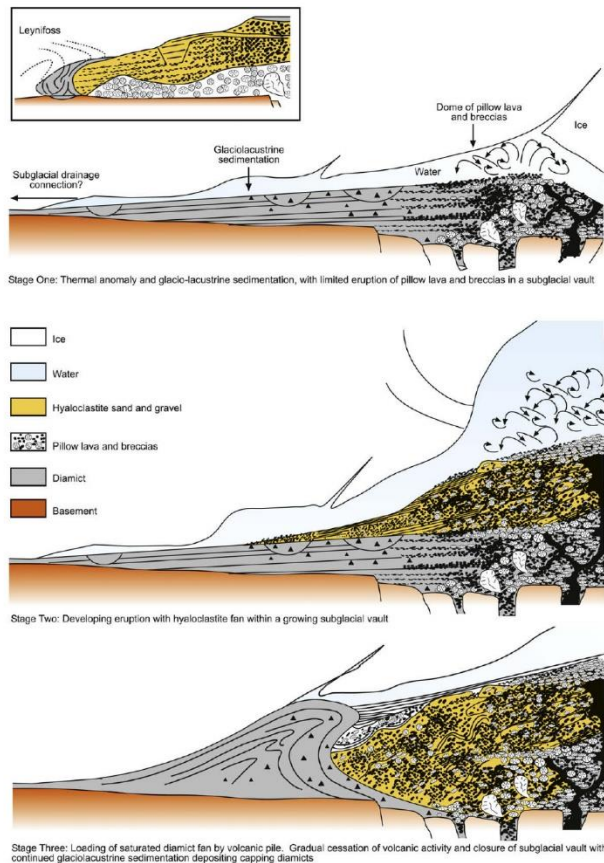
Figure 14. Schematic diagram illustrating a model for creating the deformation structures observed in glaciolacustrine englacial cavity deposits at Brekknafjöll (Bennett et al., 2009, fig. 19). The view is transverse to the tindar ridge axis.

An additional volcano-sedimentary deposit at **Arnarþúfur**, near Bláfjöll, south-west Iceland, was described by Hamilton (2004). It is less well characterized but may also be an englacial cavity sequence associated with a small active glaciovolcano. The deposit is narrow, thin and thus ribbon-like (Fig. 15). It is sourced in a small tuff cone (Vífilsfell) c. 1 km in basal diameter from which the Arnarþúfur deposit extends > 4 km. The Arnarþúfur outcrop is < 0.5 km wide, elongate and tapers in a north-westerly direction. The tuff cone sits on top of a southwest—northeast elongated fissure-erupted tindar and tuya formed of explosively generated lapilli tuff, pāhoehoe lava and volcanic breccia. The tindar was constructed on top of a poorly exposed, low-elevation pillow lava mound that was probably formed coeval with the tindar, and the tindar locally evolved into the flat-topped tuya, with its lava-fed deltas. The tindar/tuya was eroded by ice prior to eruption of the young tuff cone outcrop at the summit. Vífilsfell, which was also erupted subglacially, is a conical mound composed of thinly stratified, palagonite-altered lapilli tuff with peripheral slump deposits. The summit is c. 200 m above the surrounding lava plain. Quaquaversal bedding defines a single central

17

vent and the presence of bombs lacking well-defined impact structures suggests that eruption and deposition were subaqueous. A wet tephra pile is also indicated by the pervasive palagonitization and dykes with pillowed margins, but the presence of welded scoria interbedded with lapilli tuff in the summit crater implies that subaerial activity
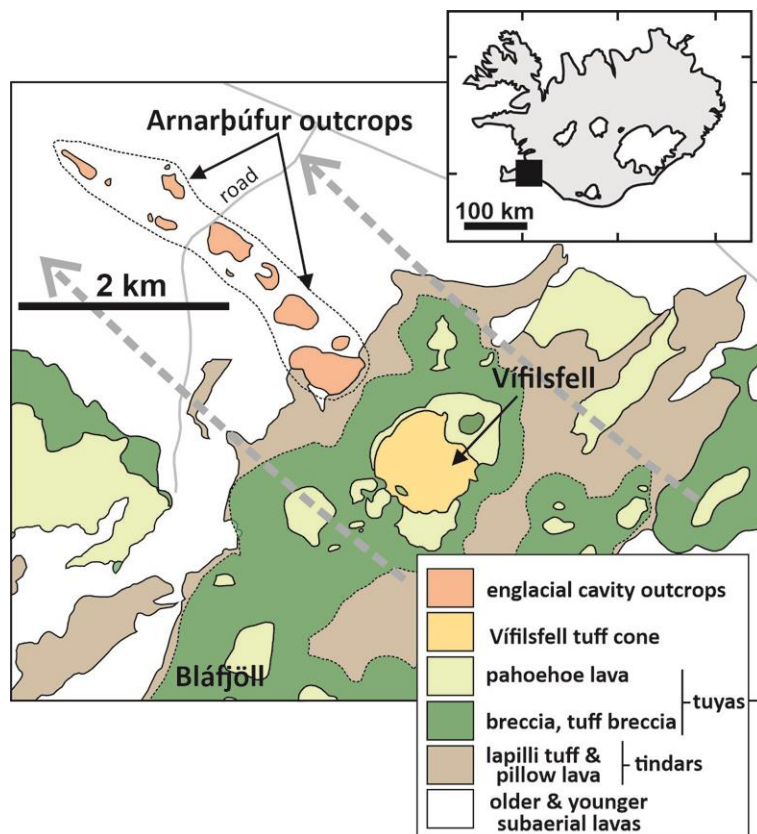
Figure 15. Simplified geological map of the Bláfjöll—Vífilsfell–Arnarþúfur area, south-west Iceland (modified after the Geological Survey of Iceland (http://jardfraedikort.is/?coordinate=64.23%2C-20.45&zoom=3) and Hamilton, 2004), showing the locations of known outcrops of putative englacial cavity (glaciolacustrine) deposits. The outcrops of breccia/tuff breccia of the lava-fed deltas (tuya edifices) are a best-estimate. Palaeo-ice sheet flow lines (grey arrows) after Hamilton (2004) and Schopka et al.(2006). The inset shows the location of the map within Iceland.

ultimately occurred. Although the tuff cone outcrop is approximately circular in plan view, it is asymmetrical in elevation (steep and taller to the ESE, gently tapered and lower to the WNW) and aligned northwest—southeast parallel to the prevailing coeval ice flow direction (flow to the north-west; Hamilton, 2004; Schopka et al., 2006). The summit of Vífilsfell is horseshoe shaped and opens into a channel on its south-west side, which curves round to the north-west with distance. The Arnarþúfur outcrop consists of several small relict mounds 20-30 m high composed of lapilli tuff similar to Vífilsfell (Fig. 15). Climbing ripples and current flutes are locally common and suggest north-westerly palaeoflow. The stratification is mound-like, with dips pointing symmetrically away from the central outcrop axis, to the north-east and south-west, but bedding orientations are commonly disturbed. The outcrops become finer grained and the clasts are more abraded in a north-westerly direction. The predominant thinly planar stratified lithofacies is closely comparable with that shown by pyroclastic density currents (cf. Branney and Kokelaar, 2002), but deposited subaqueously. Hamilton (2004) inferred that the once-continuous Arnarþúfur outcrops were deposited within a subglacial drainage channel coeval with eruption of the Vífilsfell tuff cone. The presence of abundant armoured lapilli (ash-coated lapilli?; Brown et al., 2012)

indicates that eruptions at the tuff cone had a subaerial plume prior to incorporation of the lapilli (following column collapse?) in subaqueous sediment gravity flows in the Arnarþúfur ice tunnel. Inward-dipping beds on the margins of the outcrops (also seen in edifice-marginal glaciolacustrine deposits at Brekknafjöll—Jarlhettur, described above; Bennett et al., 2006) suggest either centroclinal flow or the beds were banked up against the ice wall margins of the tunnel. The location of the ice tunnel relative to Vífilsfell and its north-westerly elongation are also consistent with deposition in an englacial cavity caused by ice flow in that direction, across a warm active volcanic mound, which supplied the abundant juvenile debris. It is therefore regarded here as a subaqueous englacial ice cavity deposit associated with active glaciovolcanism. It is suggested that the Arnarþúfur deposit is similar to broadly analogous deposits at Brekknafjöll—Jarlhettur.

The only other published example known to the author of sedimentary rocks potentially deposited in an ice cavity setting are associated with a felsic tuya at **Rauðufossafjöll**, Iceland (Tuffen et al., 2002). The outcrop is a 15 m-thick sequence of pumiceous gravelly sandstone, a basal polymict diamict and rhyolitic (including obsidian) breccias deposited variably by traction currents, hyperconcentrated flows, debris flows and rock avalanche. The sequence is only exposed on one flank of the felsic tuya and exposure is laterally very limited. Beds dip at 20-30° away from the tuya and they occupy a channel cut into felsic ash. The uppermost bed is a rhyolite breccia inferred to be derived by gravitational collapse of a nearby rhyolite lava dome, thus linking sediment deposition with construction (eruption) of the tuya, but the relationships are not clearly exposed. It was postulated that deposition fluctuated between subaerial and subaqueous, presumably in an ice tunnel marginal to the volcanic edifice. Deposition was therefore in an englacial cavity. Despite the differences in composition and their much smaller development at Rauðufossafjöll, there is a crude resemblance in structural position and depositional processes to the mafic-composition fan deposits at Laugarvatn and Brekknafjöll—Jarlhettur. Other examples of englacial cavity sediments associated with glaciovolcanism must exist elsewhere but it is remarkable that so few examples have been noticed and published, a conundrum that requires explanation.

Jökulhlaup deposits

Glacierized landscapes are frequently affected by outburst floods known as jökulhlaups, the sedimentary products of which create vast proglacial outwash plains known as sandar (singular: sandur; Björnsson, 2002; Tweed and Russell, 1999; Carrivick and Tweed, 2019). The floods form in three principal ways: (1) as enhanced runoff following storms, which results in moderate-magnitude flows; (2) from the sudden drainage of glacier-impounded lakes; and (3) as a result of glaciovolcanic eruptions. Floods from category (2) and (3) events are large magnitude and often described as catastrophic. They include the largest freshwater floods in Earth history, with volumes and discharges exceeding 10^6 m^{3}s^{-1} (e.g. Baker et al., 1993; Carrivick et al., 2004b; Alho et al., 2005; Carrivick, 2007). Jökulhlaups from ice-dammed lake-draining events are sometimes called limno-glacial whilst those associated with glaciovolcanic eruptions are referred to as volcano-glacial (Maizels, 1989, 1993, 1997). They may also be called limnogenic and volcanogenic, respectively (Jónsson, 1982; Russell et al., 2010a; Pagneux et al., 2019). Although limno-glacial jökulhlaups are associated with the largest floods (e.g. the Pleistocene Altai outburst flood of c. 18 x 10^6 m^{3}s^{-1}; Baker et al., 1993), those associated with volcanism can also be significant (Carrivick and Tweed, 2019) and some jökulhlaups are named after their source volcano (e.g. Grímsvatnahlaup: Tómasson, 1975; Katlahlaup: Jónsson, 1982). The largest-known volcano-

glacial jökulhlaups occurred during the Holocene and were sourced in the Kverkfjöll volcano (northern flank of Vatnajökull, Iceland). They were routed through Jökulsá á Fjöllum and involved repeated events with discharges of 10^5–10^6 m^{3}s^{-1} (Carrivick et al., 2004b; Alho et al., 2005), although more recent studies suggest that these values are substantially overestimated (van der Bilt et al., 2021). The 1918 jökulhlaup from Katla (Iceland) reached a maximum discharge of 2.5-4.0 x 10^5 m^{3}s^{-1} (Jónsson (1982) estimated the discharge as 1.6 x 10^6 m^{3}s^{-1}), releasing a total volume of c. 8 km^3 of flood water. Although the principal flood lasted only half a day, it temporarily moved the coastline seaward by 3.6 km (Tómasson, 1996; Duller et al., 2014). Finally, the short-lived, mafic glaciovolcanic eruption of Gjálp in 1996, also in Iceland (Vatnajökull), generated a flood of 3.4 km^3 and a discharge that peaked at 5 x 10^4 m^{3}s^{-1} (Jóhannesson, 2002), equivalent to four times the discharge of the Mississippi River. It was thus briefly the second largest freshwater discharge on Earth, exceeded only by the Amazon, despite being generated by a comparatively small volcanic eruption (Smellie and Edwards, 2016, p. 81). The associated jökulhlaup also delivered more than 1.8 x 10^6 tonnes of suspended solids to the sea in only 42 hours (Tómasson, 1996; Stefánsdottir and Gíslason, 2005). This amounts to c. 1 % of the total annual suspended flux delivered by rivers globally to the oceans. Jökulhlaups with discharges less than c. 2-4 x 10^3 m^{3}s^{-1} are probably below the limits of detection within the sedimentary and landform record (Maizels, 1989).

The hydrographs of limno-glacial and volcano-glacial jökulhlaups differ. Limno-glacial hydrographs characteristically exhibit a relatively slow, gradual rise in discharge followed by a rapidly falling limb. By contrast, volcano-glacial hydrographs commence abruptly with a rapid rise to peak discharge followed by a much more gradual falling limb (Maizels, 1993; Tómasson, 1996; Jóhannesson, 2002). The hydrograph profiles are generally explained by the ability of volcanically heated meltwater to rapidly enlarge subglacial tunnels compared with much colder water sourced in glacial lakes (Björnsson, 1998; Waller et al., 2001). An over-pressured water-filled englacial cavity can also be hydraulically lifted, thus propagating a subglacial pressure wave and allowing an early peak discharge to be established (Jóhannesson, 2002; Einarsson et al., 2017), but the fundamental reasons for the differences between hydrographs are not fully understood. Hydrograph shapes can be more irregular owing to ancillary effects such as temporary blockages during tunnel collapses or constriction by ice masses in transport leading to pulsed flow (Sturm et al., 1987; Maizels, 1997; Tómasson, 1996). Jökulhlaups may even change their drainage routes as a result of substantial tunnel blockages (Tweed and Russell, 1999).

Jökulhlaups are strong geomorphological agents capable of creating substantial landforms and significantly modifying landscapes (e.g. Maizels, 1997; Carrivick et al., 2004a; Russell et al., 2010a). They are also characterized by distinctive features such as kettles and ice-block obstacle marks (Maizels, 1992; Branney and Gilbert, 1995; Russell et al., 2000; Fay, 2002a,b; Everest and Bradwell, 2003; Roberts and Gudmundsson, 2015), which are diagnostic of jökulhlaups. Kettles can survive for decades to hundreds of years (Fig. 16; Everest and Bradwell, 2003; Roberts and Gudmundsson, 2015) and they can leave a distinctive imprint in the geological record (Maizels, 1992; Olszewski and Weckwerth, 1999; Russell et al., 2010a; Smellie et al., 2016). Moreover, because of the actual and potential economic damage and loss of human lives associated with jökulhlaups, their triggers, progress, processes involved and the resulting sedimentary products and landforms are well studied and there is a large published literature (e.g. Jónsson, 1982; Maizels, 1989, 1993, 1997; Tómasson , 1996;

Gudmundsson et al., 1997; Tweed and Russell, 1999; Carrivick et al., 2004a,b, 2007; Elíasson et al., 2006, 2007; Russell et al., 2006, 2010a; Komatsu et al., 2007b; Duller et al., 2008, 2014; Marren et al., 2009; Pagneux et al., 2015). Much of it is focussed on the outwash plains (sandar) of southern Iceland, which extend for tens of kilometres from the margins of
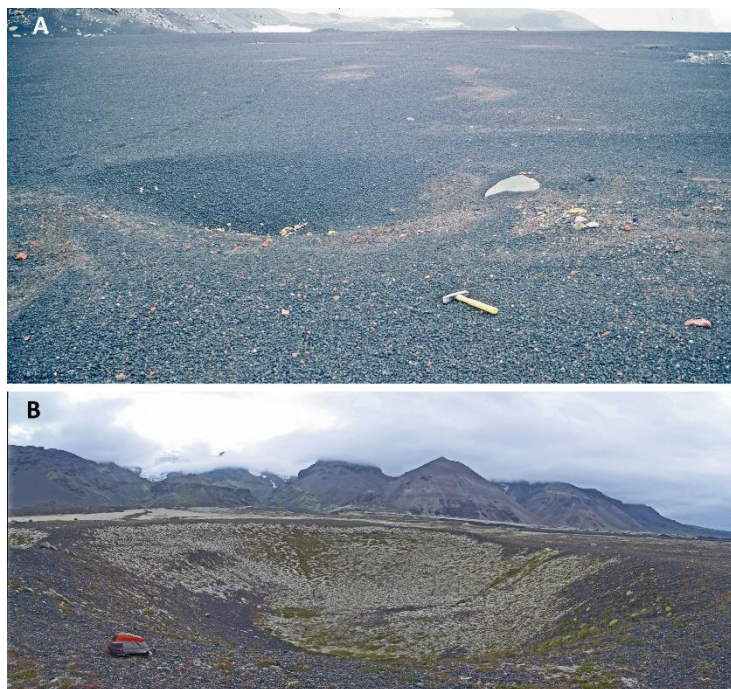
Figure 16. Photographs of kettles formed from buried ice preserved in historical jökulhlaup deposits, illustrating how resistant such ice-block structures can be to removal by erosion. A. Small kettle in a deposit on Deception Island (Antarctica) formed during the 1969 glaciovolcanic eruption of Mt Pond (see Smellie, 2002), photographed in 1995; the kettle is c. 3 m in diameter. B. Large kettle in the Kotá fan (Iceland), measuring c. 70 m in diameter, formed during a major jökulhlaup associated with the 1727 glaciovolcanic eruption of Öræfajökull (see Roberts and Gudmundsson, 2015), photographed in 2013.

ice caps and glaciers. Numerous papers have established the range of lithofacies deposited by jökulhlaups (e.g. Maizels, 1989, 1993, 1997; Carrivick et al., 2004b; Marren et al., 2009; Russell et al., 2010a; Duller et al., 2006, 2009). Observed and modelled jökulhlaups show that they can be extraordinarily extensive, rapid and deep over large areas. For example, the 1918 Katlahlaup inundated the full width of Mýrdalsandur and had calculated mid-sandur flow depths of 20-30 m (Maizels, 1993; Tómasson, 1996). Modelled Katlahlaups are also capable of inundating the Markarfljót valley in only 10 hours, with modelled flow depths of 20-25 m proximally, diminishing to 10 m by the coast (Elíasson et al., 2007). The volume of meltwater discharged correlates with eruption magnitude and duration (Jónsson, 1982; Tómasson, 1996; Russell et al., 2010a). Jökulhlaups suddenly entering the sea can also create tsunami (Elíasson, 2008). Present-day rivers on Iceland's sandar are misfits that cannot explain the large-scale erosional features and depositional volumes observed (Russell et al., 2010a).

In this paper the focus is only on volcano-glacial jökulhlaups and their associated sediments. A key condition for the generation of these jökulhlaups is the temporary impoundment of meltwater in a subglacial vault, the sudden release of which causes a jökulhlaup. Jökulhlaups are therefore restricted to ice-covered volcanoes, i.e. those in which the thickness of ice above the vent is > c. 200 m (Fig. 2). Volcano-glacial jökulhlaup deposits are generally distinguished by an overwhelming abundance of fresh juvenile detritus, typically

sideromelane derived from the explosive hydrovolcanic eruptions that caused the melting and ultimately triggered the jökulhlaups. Jökulhlaups associated with tuya eruptions have never been observed. Although it has been inferred that they must occur (Björnsson, 1988), the conditions for lava-fed delta formation (i.e. advancement into ice-impounded water) generally preclude the flotation of the surrounding ice and sudden release of large volumes of water. Conversely, limno-glacial jökulhlaup deposits are polymict. They also usually contain a large percentage of abraded cobbles and boulders, whereas volcano-glacial jökulhlaup deposits are dominated by (juvenile) sand and fine gravel grain sizes, which also have less abraded shapes. Volcano-glacial jökulhlaups can also incorporate debris from the bedrock and regolith over which they passed (Fig. 17a,b), although the proportion of debris

Figure 17. A. View of the surface of a jökulhlaup fan deposit on Sólheimasandur. The surface is strewn with numerous indurated lapilli tuff blocks and abraded lava boulders derived by bedrock erosion during a jökulhlaup event. B. Large bedrock clast deposited by the same jökulhlaup event shown in (A). Jim Head (1.8 m) for scale. C. Lava block 2 m in diameter deposited by the 1969 jökulhlaup on Deception Island, photographed in 1995. Note the moat surrounding the block, excavated by the water flow (from right to left), still preserved 25 years after the event. D. Till mounds up to c. 10 m in width left by the 1969 jökulhlaup on Deception Island, photographed in 1995. The mounds represents formerly frozen debris torn from the base of the Mt Pond glacier during the jökulhlaup.

is generally minor overall apart from in early-formed flows in proximal areas (close to the ice terminus). The sizes of blocks carried and deposited by jökulhlaups can be impressively large (up to 1000 tons, carried over 14 km; Jónsson, 1982; Russell et al., 2010a; Fig. 17b,c) and they can include large blocks of frozen basal till, left behind as till mounds (Fig. 17d). Bedrock erosion is enhanced by jökulhlaups that occur within confined, steep bedrock channel systems, and substrate-derived (bedrock and regolith) and non-juvenile debris is prominent (Carrivick et al., 2004b). The debris is recognized by its polymict nature, often crystalline rather than glassy, rich in palagonite (a pervasive clay alteration mineral of mafic sideromelane), and abraded clast shapes. Also, in some cases such as jökulhlaups linked to Grímsvötn (Grímsvatnahlaups), a jökulhlaup may be sourced in a subglacial lake that is simply a holding tank for meltwater derived from a glaciovolcanic eruption located elsewhere within the catchment area. Thus, the clastic content of Grímsvatnahlaups mainly

reflects debris contained in the subglacial Grímsvötn caldera and picked up en route to the ice terminus rather than that produced at the eruptive site. Because deposits of jökulhlaups have been investigated and described by sedimentologists in recognition of the sedimentary setting, epiclastic terminology has invariably been used. However, they are largely composed of the redeposited unconsolidated products of explosive glaciovolcanic eruptions and are thus syn-eruptive (cf. McPhie et al. (1993). Similar to our argument for englacial cavity (glaciolacustrine fan) deposits, above, they are therefore often predominantly volcaniclastic rather than epiclastic (sensu White and Houghton, 2006). Moreover, analogous jökulhlaup lithofacies called glaciovolcanic sheet-like sequences (Smellie, 2008) that were deposited under the coeval ice and not on the sandur have been described by most volcanologists using volcaniclastic terminology (Walker and Blake, 1966; Bergh, 1985; Berg and Sigvaldason, 1991; Sigvaldason, 1992; Smellie et al., 1993; Smellie, 2008; Banik et al., 2014; but not Loughlin, 2002). A dichotomy therefore exists between proximal (sub-ice) and distal (sandur) jökulhlaup deposits from the same event(s) being described using contrasting terminology. In this paper, we recognise that epiclastic terminology is embedded in a very extensive literature for the sandur deposits. It is therefore retained and used here for the sandur successions in order to facilitate comparison with the large jökulhlaup literature and avoid unnecessary confusion. However, the use of volcaniclastic terminology is retained for the more proximal sub-ice equivalents known as sheet-like sequences (see later).

Distal jökulhlaup deposits (1) – sandar plains

Distal deposits are described first because they are so well studied. Volcano-glacial jökulhlaup deposits are most widely developed on sandur plain and valley sandar where they typically comprise ≥ 85 % of the preserved sediment (Fig. 18; Maizels, 1989; Gomez et al., 2000). They construct braided sediment trains and fans. The latter issue from marginal

Figure 18. Aerial views of Icelandic sandar. A. braided sandur plain (Skeiðarársandur) and B. valley sandur (Sprengisandur).

valleys and often show axial dissection caused by late-stage waning flood conditions as well as by later 'normal' fluvial dissection unrelated to jökulhlaups. This results in prominent

lateral terraces, particularly at the fan apex, indicating discrete stages of baseline readjustment linked to late-waning and post-flood incision (Fig. 19). The erosional and depositional impacts of jökulhlaups diminish with distance downstream, as do the number and sizes of boulders and ice blocks (Russell et al., 2010a). Many lithofacies have been

Figure 19. View looking towards the apex of the Kotá fan (south-west flank of Öræfajökull), formed during a jökulhlaup in 1727. The jökulhlaup issued from Kotárjökull via the two prominent gullies flanking Slaga. The resulting fan has been extensively modified, probably during the late stages of the jökulhlaup event, when the prominent terraces seen near the fan apex at right were incised, as well as during normal post-jökulhlaup stream flow. As a result of late- and post-jökulhlaup sediment redistribution, fan and sandar surfaces formed during jökulhlaups can be significantly lowered (Harrison et al., 2019).

identified in volcano-glacial jökulhlaup deposits, but one lithofacies association is ubiquitous and characterizes the main flood event (often called a surge) in its principal channel(s). Where fully developed, it is tripartite, comprising pre-surge and post-surge gravels with fluid-flow bedforms which bookend a central thicker deposit of massive sandy gravel deposited mainly by hyperconcentrated flows (Fig. 20). However, more recent studies, based on three-dimensional exposures rather than the one-dimensional vertical profile sections used by Maizels (1989, 1993, 1997), have convincingly demonstrated that the main flow event in the 1918 Katla jökulhlaup was supercritical, characterized by multiple large migrating antidunes deposited from highly concentrated fluidal flows rather than hyperconcentrated flows (Duller et al., 2008, 2014; Russell et al., 2010a). The faint curviplanar stratification illustrated by Maizels (1993, fig. 6a) is consistent with that interpretation. Although antidunes are sometimes mentioned by others for other jökulhlaups, based on landforms (e.g. Alho et al., 2005; Marren et al., 2009; Russell et al., 2010a), it is not known how common they are relative to hyperconcentrated flow deposits and what the typical flow rheology is for jökulhlaups. Both flow modes have been inferred for some jökulhlaups (Russell et al, 2010a).

The 'core' lithofacies association of sandur deposits ('Type B3 profile' and variants of Maizels, 1997; Fig. 20) is dominant in large areas of the volcano-glacial sandurs. Individual complete deposits can exceed 12 m in thickness, mostly composed of massive granule-grade gravel sometimes showing faint stratification mainly to base and top. The underlying and overlying gravels may be absent, forming truncated lithofacies associations ('marginal flows' in Fig. 20). The basal gravels are < 2 m thick and crudely horizontally to rarely trough cross-bedded. The capping trough-cross stratified and planar stratified gravels are typically 1-3 m thick, with channels up to 11.5 m wide and 1.4 m deep. The core lithofacies association was
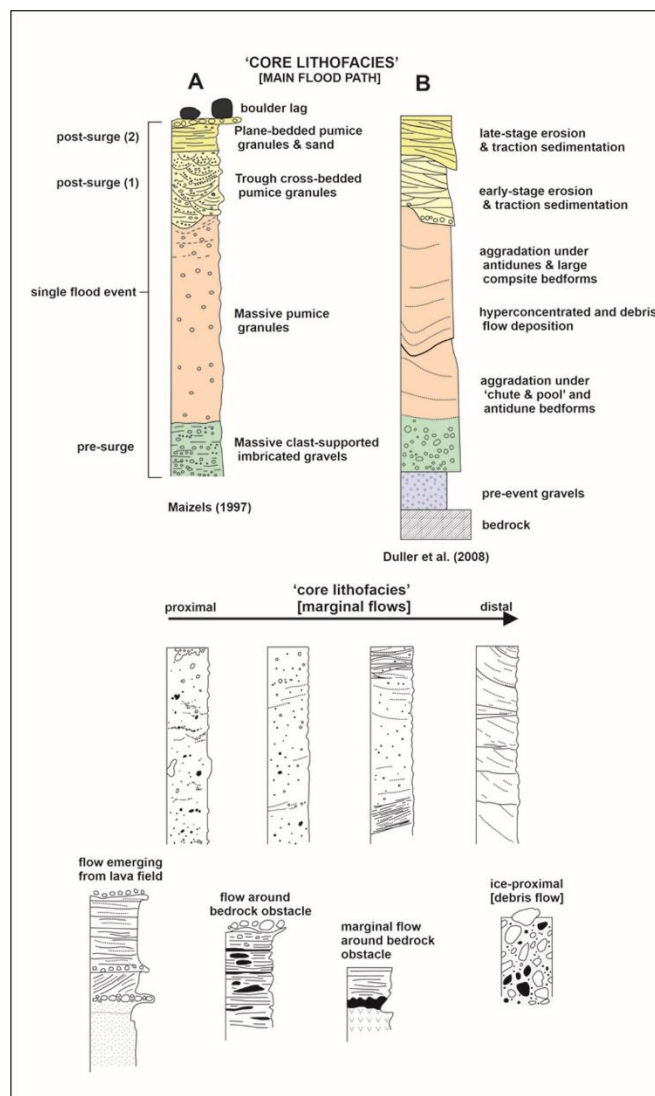
Figure 20. Schematic vertical profile sections through lithofacies characteristic of jökulhlaup deposits on sandar plains (after Maizels, 1989, 1993, 1997; Duller et al., 2008). The 'core lithofacies' represents deposits of the main flood path and is representative of the bulk of the jökulhlaup deposits. It has been interpreted variably as a deposit of hyperconcentrated or supercritical flow. Numerous lithofacies variations also occur depending on the depositional location relative to the main flow path (other profile sections shown; see text for description).

deposited mainly from hyperconcentrated flows or antidunes. It was laid down from the main flood surge and is dominated by juvenile volcanic clasts (typically black when associated with mafic eruptions) derived by syn-eruptive redeposition of glaciovolcanic tephras, together with a small proportion of locally derived bedrock or surface regolith seen mainly in ice-proximal outcrops. The basal lithofacies, with its crude planar stratification, accumulated ahead of the main surge ('pre-surge' of Maizels, 1997). It was deposited rapidly from suspension or hyperconcentrated flow conditions, contains a high proportion of reworked sandur gravel and is associated with the initial rapidly rising surge flood. By contrast, the upper stratified lithofacies represents waning flow, post-surge conditions. It marks a distinct upward transition from hyperconcentrated or antidune flow of the main surge phase to rapid traction flows characterized by smaller migrating dunes (trough cross beds) or, at lower flow velocities, planar stratified beds deposited from shallow fluctuating

sheet flows. While still containing relatively high sediment concentrations, the upper stratified deposits represent the declining competence and tractive power of fluid flows.

A wide array of additional lithofacies has also been recognized (e.g. Maizels, 1989, 1993; Carrivick et al., 2004b; Duller et al., 2004; Russell and Knudsen, 1999; Russell et al., 2006, 2010a). They are of lesser volumetric importance compared to the core lithofacies and primarily illustrate the consequences of local flow conditions on the resulting deposits, e.g. associated with flow margin effects, bedrock obstacles, slack water, ice-proximality (debris flow deposits), cobble- and boulder-rich lags, remobilisation of earlier debris lobes, or whether the flood waters were (temporarily) moraine confined (Gomez et al., 2000; Russell et al., 2006; Fig. 20). The succession of depositional processes and related bedforms are unique to specific locations and hydrodynamic conditions on a sandur and its configuration, thus yielding substantial spatial variability in terms of the vertical lithofacies associations and overall sedimentary architecture (Duller et al., 2008; Russell et al., 2010a). The subsidiary lithofacies are not further described here.

The deposits create large depositional landforms categorized as sandur plains, valley sandar and outwash fans (Maizels, 1997). Large-scale erosional as well as depositional forms are present, including streamlined residual hills, longitudinal grooves, giant potholes, scours and plunge pools, and spillways, sediment bars, dunes, boulder lags, pitted and kettled outwash, obstacle marks and a variety of proximal fans. Together, they define a distinctive array of landforms that characterize a jökulhlaup landsystem (Fig. 21).
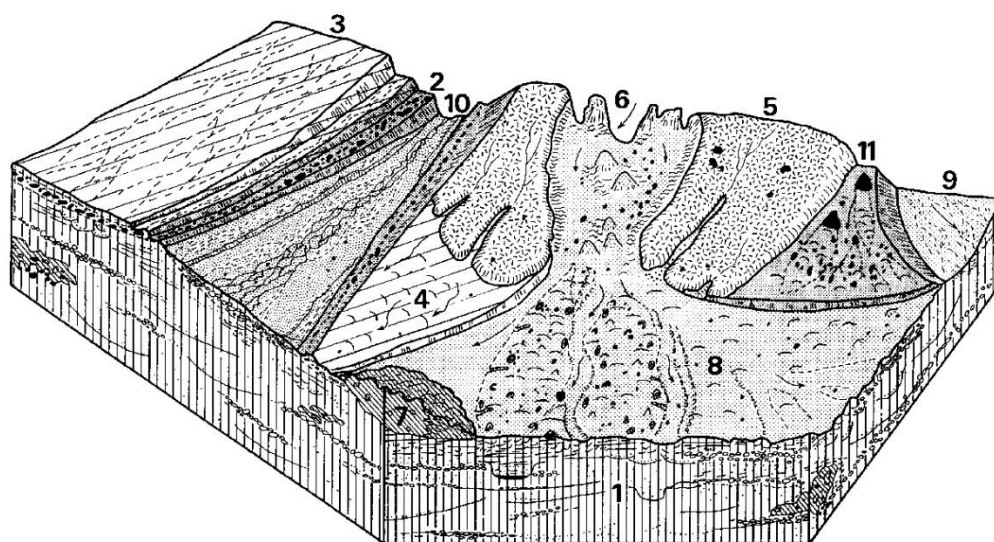
Figure 21. Model summarizing a sandur landsystem subject to volcano-glacial jökulhlaups showing the sedimentary deposits and landforms created (from Maizels, 1997). 1 – stacked sequences of multistage massive granular sediments; 2 – terraced boulder deposits; 3 – high-level, abandoned sandur surface exhibiting thin gravel horizon and braided palaeochannel networks; 4 – 'washed' sandur; 5 – lobate fan deposited by hyperconcentrated jökulhlaup flows; 6 – incised jökulhlaup channel with streamlined residual hummocks, boulders and megaripples; 7 – hummocky distal jökulhlaup deposit; 8 – streamlined, hummocky residual bars mantled with rimmed and till-fill kettles; 9 – incised jökulhlaup channel; 10 – incised meltwater channel; 11 – streamlined erosional bars, wash limits and scattered boulders and dune forms downstream of bedrock obstacles. Several of the features labelled are seen in Figure 19 (particularly examples of features 2, 3 and 10), which also provides a natural example of the scale of the features shown in this diagram. See Maizels (1997) for further detailed description.

Distal Jökulhlaup deposits (2) – confined channel systems

Two broad categories of jökulhlaup-related deposits have been defined for confined channel systems (canyon-forming jökulhlaups) in northern Iceland (Jökulsá á Fjöllum) fed by volcanic eruptions beneath Vatnajökull sourced particularly in the Kverkfjöll volcano (Carrivick et al., 2004b): (1) main valley fill and (2) tributary mouth, the latter representing slack water deposits, i.e. deposits laid down by backed-up flows originating in the main drainage channel. The sediments in both categories are more spatially variable and less regularly structured than displayed by unconfined jökulhlaup deposits of the sandar, although the depositional processes are similar (Fig. 22a,b). The variability implies an absence of laterally uniform flow conditions. Abrupt changes to the flow hydraulics or sediment supply are
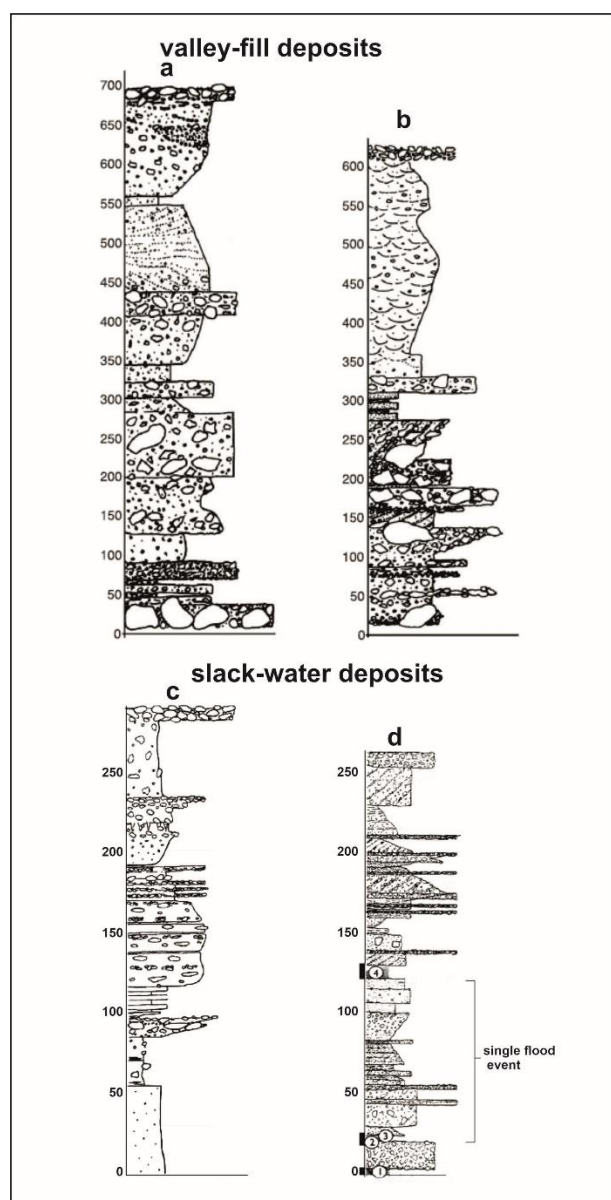
Figure 22. Sedimentary logs of lithofacies characteristic of jökulhlaup deposits of confined channel systems (after Carrivick et al., 2004b). Because of the rapid lithofacies variations, it can be difficult to distinguish deposits of individual jökulhlaup events (only identified in one log). The depositional processes occurring in channel-confined systems are essentially similar to those shown by jökulhlaup deposits of sandar plains but the deposits are much more variable.

inferred consistent with a multi-event or multi-pulse origin for the deposits that makes it hard to distinguish between successive jökulhlaups (Carrivick et al., 2004b). The valley-filling sediments (broadly equivalent to the 'core lithofacies' of sandar) are dominated by massive to inverse-graded products of hyperconcentrated flows (matrix supported) varying to more fluidal flows (clast supported), together with planar-bedded ungraded units representing a migration toward late-stage traction transport. Less common beds are horizontally bedded massive silt and sand, some associated with scour and fill, suggesting upper- and lower-flow tractional regimes. Dipping beds probably represent the passage of migrating shallow-relief bedforms. The slack-water deposits show particularly pronounced spatial (vertical and lateral) variability compared with lithofacies of the main channel (Fig. 22c,d). They are finer-grained and thinner-bedded but are interpreted similarly to the main channel deposits, or to pulses in sediment supply or flow conditions within single depositional events. Dipping beds (Fig. 22d) represent shallow-relief bedforms that prograded up the tributary valley indicating flow away from the main channel. Deposits in both settings contain abundant polymict debris reflecting multiple sediment sources.

Proximal (subglacial) jökulhlaup deposits - glaciovolcanic sheet-like sequences

Sheet-like sequences are a distinctive category within glaciovolcanism (Loughlin, 2002; Smellie, 2008, 2009, 2013). As the name implies, they occur as laterally extensive sheets and narrow ribbon-like (valley-confined) outcrops probably erupted from fissures and isolated centres, respectively. Although two discrete types of deposit were suggested and known as Dalsheidi- and Mt Pinafore-types (Smellie, 2008), they were later recombined into a single type by Smellie and Edwards (2016) based on acknowledgment of the substantial similarities in lithofacies, although there is a noticeable difference in scale between the two types. Examples are widely distributed in Iceland (e.g. between Eyjafjallajökull and Öræfajökull) but are much less common elsewhere in the world (Antarctica: Smellie et al., 1993, 2011a).

Sheet-like outcrops: The most detailed study is by Bergh (1985; also Bergh and Sigvaldason, 1991) for extensive outcrops in the Sida—Fljotsfverfi district of south-east Iceland. Using lithofacies analysis, Bergh (1985) was able to define a standard depositional unit that is repeated time and again during successive eruptions (Figs 23, 24). Ignoring the presence of generally thin glacial sedimentary deposits beneath many of the volcanic units, which were used by Bergh (1985) to make lateral correlations, the standard unit is tripartite. From base up, it is formed of (1) lava showing spectacular columnar jointing of colonnade, entablature and kubbaberg (including hackly or blocky types; see Forbes et al., 2014, for explanation of jointing types and how they form); (2) a central voluminous thick deposit of mainly massive lapilli tuff and tuff; and (3) an upper thin unit of stratified tuff. Variations on the standard depositional unit also occur, consisting of sequences lacking one or more of the constituent lithofacies (Fig. 23b-d). Bergh (1985) demonstrated that outcrops closer to source (i.e. unvisited eruptive fissures inland) are dominated by the basal lava, which Smellie (2008) named an interface sill because it shows abundant evidence for intrusion into the host lapilli tuff and tuff, which were wet at the time (see Smellie and Edwards, 2016, for further description); it shall not be further described here. The clastic deposits are dominated by lapilli tuff and tuff (hereafter simply called lapilli tuff for convenience), 10-120 m thick (average: c. 40 m), which form at least two thirds of each deposit. Calculated volumes for the individual sequences are impressively large. They are mostly > 10 km^3, with mean volumes (including interface sills) ranging from c. 0.1 to 31.4 km^3 (average: 12.6 km^3; Bergh,

1985) but the estimates depend on the validity of the mapping, which has not been
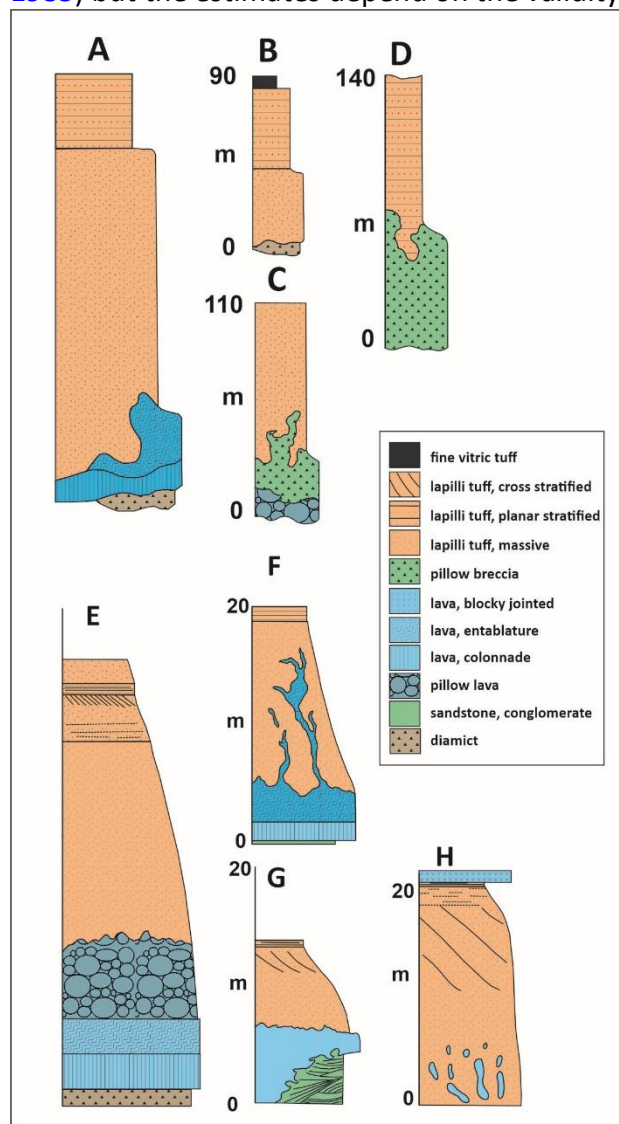
Figure 23. A. Selected representative vertical profile sections of sheet-like sequences for laterally extensive sheet-like (A-D) and valley confined (E-H) outcrops, respectively (modified after Bergh, 1985 and Loughlin, 2002). Profiles A (based on Sida—Fljotsfverfi district) and E (based on Eyjafjallajökull) depict standard depositional units identified by Bergh (1985) and Loughlin (2002), respectively; the vertical scale is exaggerated in both, for clarity. The other profiles shown are variants of the two standard depositional units. Note the very different vertical scales for deposits in the two settings, despite the similarities in lithofacies.

rigorously tested. The lapilli tuff is mainly massive, with a relatively uniform or upward-decreasing grain size and faint crude planar stratification to top. The normal grading described by Bergh (1985) is not prominent but is emphasized by basal deposits that are often rich in coarse fragments spalled off the chilled basal sill mingled with lapilli tuff. The lapilli tuff rapidly fines up into the upper tuffs showing planar or much rarer cross stratification. The sequence is interpreted to represent transport and deposition mainly from a hyperconcentrated flow (massive deposit), with the flow becoming somewhat less concentrated upward and developing minor traction structures (crude stratification). The capping unit of stratified tuffs represents the final waning depletive stage of the current, with the planar stratified part representing upper flow stage traction deposition, and the rarer cross stratification indicating the migration of dune bedforms.
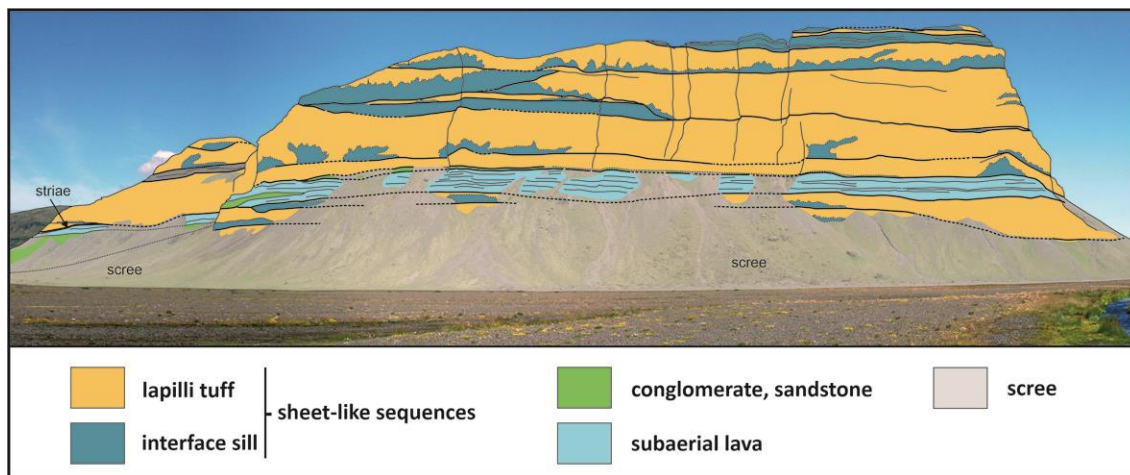
Figure 24. Sketch of multiple interbedded sheet-like sequences at Lomagnúpur, southern Iceland. Of Pliocene or early Quaternary age, each sequence represents the products of a single jökulhlaup event linked to relatively voluminous glaciovolcanic fissure eruptions, including an intrusive basal sill (interface sill of Smellie, 2008). The clastic units represent the proximal subglacial equivalents of subaerially-emplaced jökulhlaup deposits on the sandar. The exposed cliff face is c. 500 m high. Based on Smellie, unpublished.

The overall similarity of the clastic standard sheet-like sequence to the tripartite core lithofacies of sandur jökulhlaups identified by Maizels (1989, 1993, 1998) is obvious (cf. Figs 20, 23). Larsen (2000) described a possible sheet-like sequence that exited Kötlujökull (a glacier on the east flank of Katla) and was thus subaerial, although the field relationships were described as ambiguous by the author. Banik et al. (2014) also postulated that some of the sheet-like sequences described by Bergh (1985) were subaerial, at least in part, but without providing evidence. Here, it is suggested that glaciovolcanic sheet-like sequences are mainly the subglacial equivalents of the sandar jökulhlaups. They are therefore regarded as the proximal (subglacial) and distal (subaerial) equivalents, respectively, of the same events. One possible difference may be that the interface sill of sheet-like sequences is absent from the subaerial jökulhlaup sequences, or at least no convincing example has yet been described. However, Sigvaldason (1992) described a sheet-like sequence at Dyngjufjöll Ytri, west of Askja (north-central Iceland). The sequence contains a basal sill but the surface of the deposit is strewn with numerous (> 1300) tiny crater-like structures, 2-50 m in diameter and up to 6 m deep, that were interpreted as much younger explosion vents caused by hydrothermal activity related to the migration of a non-eruptive volcanic fissure below the area. The hypothesis has several possible flaws, including how the craters can consist of fresh sideromelane particles that were supposedly derived explosively from the underlying, supposedly much older, strongly lithified (palagonitized) lapilli tuff of the sheet-like sequence, and why the craters show no clear ejecta blankets but comprise narrow rings of blocky debris (not further described; see Sigvaldason, 1992, fig. 7). However, another explanation is possible for the Dyngjufjöll Ytri occurrence. From satellite images, the crater-like rings are seen to vary from examples with broad raised rims and shallow interiors, to others with narrow rims and deeper interiors. They are also irregular in outline, with coalesced shapes commonly present (acknowledged by Sigvaldason, 1992; Fig. 25). In size, morphology and, possibly, clast characteristics, the craters have a remarkable resemblance to boulder ring structures formed by the decay of debris-rich ice blocks released during subaerial jökulhlaups (see Maizels, 1992, figs 3 and 4a; also Russell et al., 2010a, fig. 11.15). Moreover, both Sigvaldason (1992) and Maizels (1992) comment on how the interiors of the crater structures they describe are noticeably paler than their surroundings. Thus, if the

crater structures at Dyngjufjöll Ytri are boulder rings and they are cogenetic with the underlying sheet-like sequence, the latter was emplaced subaerially.
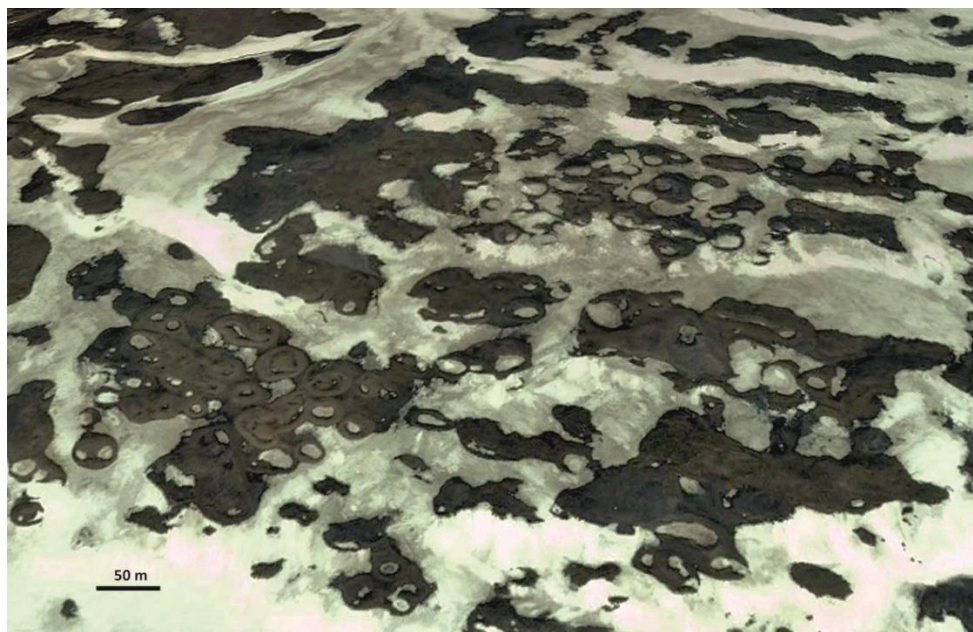
Figure 25. Satellite image perspective view of part of the surface of Dyngjufjöll Ytri showing multiple small crater-like features, described as hydrothermal explosion craters (Sigvaldason, 1992). The scale shown is approximate. See text for description. The features are reinterpreted here as boulder ring structures (sensu Maizels, 1992) associated with the melting of surface-strewn ice-blocks following a major jökulhlaup event possibly represented by the underlying glaciovolcanic sheet-like sequence. Image: Google Earth and Maxar Technologies (2021).

Valley-confined outcrops: The narrow ribbon-like glaciovolcanic sheet-like sequences are described in detail by Walker and Blake (1966), Loughlin (2002) and Smellie et al. (1993). They appear to have formed within pre-existing subglacial valleys (i.e. valley-confined), whereas the laterally more extensive sheet-like sequences described above both fill and extend well outside of any pre-existing valleys (Bergh, 1985). It seems likely that the valley-confined ribbon-like outcrops are related to much smaller-volume volcanic eruptions, probably from point sources rather than fissures. Like the lithofacies produced by subaerial jökulhlaups in confined channel systems, the lithofacies in the ribbon-like outcrops are similar to those described by Bergh (1985) but form thinner beds and the lithofacies relationships are more variable. This is particularly well shown by Loughlin (2002), who identified at least nine different lithofacies associations for examples on Eyjafjallajökull (south Iceland), although there is a tripartite 'core association' common to all that is essentially comparable with that established by Bergh (1985; cf. Fig. 23). However, by contrast to valley-confined jökulhlaup deposits, the valley-confined sheet-like sequences described so far are monomict apart from some thin basal sediments laid down ahead of the main surge phase (Smellie et al., 1993). They probably will generate a jökulhlaup sediment fan where they exit the glacier snout and spread out onto the adjacent sandur, probably similar in appearance to the Kotá and Skógá fans in southern Iceland (Maizels, 1989, 1993; Fig. 19).

Lahar deposits

Eruptions at ice-capped volcanoes also have the potential for rapidly melting large volumes of snow and ice, and generating a wide variety of mass flow events, including debris

avalanches, avalanches of snow and ice, and lahars (Major and Newhall, 1989; Pierson and Janda, 1994; Pierson, 1995). Additionally volcanoes that are seasonally clad in snow can also generate lahars during eruptions, although they are rarely sizeable (Kjartansson, 1951; Major and Newhall, 1989). Lahars consist of debris flows and sediment-laden water floods, the latter also called hyperconcentrated flows or lahar runouts (Scott, 1988; Pierson and Scott, 1985; Scott et al., 1995). Like jökulhlaups, lahars occur on *active* glaciovolcanoes (Gudmundsson, 2015) but, because the summit ice (and snow, firn) is unable to impound meltwater at source, they don't typically involve outburst floods although sometimes pre-existing lakes and others temporarily impounded behind topography are overtopped by the rapid influx of eruption-induced meltwater, leading to widespread flooding (Pierson, 1999). The resulting hydrographs are essentially similar to those associated with jökulhlaups.

Primary lahars (Mothes and Vallance, 2015; Thouret et al., 2020) are composed mainly of volcanic clasts and they are a direct consequence of volcanic activity rather than simply a product of mass wasting of volcanoes in an alpine setting, such as snowmelt-induced debris flows (Scott, 1988). The deposits are conspicuously associated with stratovolcanoes scattered along the Pacific consuming plate margins of North and South America (Fig. 1). Most of the volcanoes rise to 3000-6000 metres above sea level and have steep flanks deeply dissected by streams and glaciers and their upper slopes are covered by snow and ice (Fig. 3a). Primary lahars are fast-moving (flow speeds of tens of metres.s^{-1}), often voluminous (10^7-10^9 m^3) and capable of travelling great distances, sometimes hundreds of kilometres (Pierson, 1995; Mothes and Vallance, 2015; Delgado Granados et al., 2021). For example, Cotopaxi volcano (Ecuador) has a small ice cap, 14 km^2 in area and with a total volume of just 0.5 km^3, but suffered a large-magnitude lahar in 1877 that travelled 325 km as a result of an eruption generating pyroclastic density currents (pdcs; Mothes et al., 1998; Mothes and Vallance, 2015). Peak outflows can also be similar to jökulhlaups (20-60 km^3.s^{-1}). Lahars are also generated at volcanoes lacking snow or ice, for example following rainstorms ('meteorological lahars'), and at inactive volcanoes (e.g. flank-collapse lahars and lake-breakout lahars; Huggel et al., 2007; Friele et al., 2008; Vallance and Iverson, 2015). They are known as secondary lahars (Mothes and Vallance, 2015). Secondary lahars derived from the mechanical failure of a snow-covered volcano not uncommonly have an intermediate stage of debris avalanche. They are also likely to be more clay-rich (hence cohesive) and lithic clast-rich, with minor pumice or other juvenile glass, so they should be distinguishable from primary lahar deposits (Scott et al., 1995; Friele et al., 2005; Simpson et al., 2006). Cohesive and fine matrix-rich lahars are also less easily diluted by water and are slow to transform to hyperconcentrated flows (Delgado Granados et al., 2021). Only glaciovolcanic (primary) lahars are discussed here. Although lahars are often triggered by relatively small eruptions, they may have catastrophic effects. For example, despite the comparatively small area of summit snow and ice at Nevado del Ruiz, the lahars generated in the small (VEI3) 1985 eruption were highly destructive as well as lethal because of the effective transfer of heat and energy from pyroclastic debris to the snowpack and bulking up with alluvial detritus and river water (Pierson et al., 1990; Thouret, 1990).

Because of the significant hazards they represent for human populations and infrastructure, lahars and their deposits are well studied, with an extensive literature particularly focussed on the large active North and South American stratovolcanoes (e.g. Pierson, 1985; Lowe et al., 1986; Naranjo et al., 1986; Scott, 1988; Waitt, 1989; Pierson et al., 1990; Thouret et al., 1990, 2020; Trabant et al., 1994; Scott et al., 1995; Mothes et al., 1998; Pierson and Waitt,

1999a; Huggel et al., 2007; Mothes and Vallance, 2015; Delgado Granados et al., 2021; Procter et al., 2021). Two key processes by which volcanism creates lahars are volcanic explosive activity and mass failures of lava domes (Mellors et al., 1988; Major and Newhall, 1989; Thouret, 1990; Pierson and Waitt, 1999b). During explosive eruptions, the dynamic mixing of hot pyroclastic material by turbulent high-velocity pdcs ('surges' and 'pyroclastic flows') appears to be a critical factor in transferring heat effectively. Pdcs produce voluminous lahars because they rapidly melt and entrain ice, forming an ice scabland (Waitt, 1995) or sometimes scouring glacier ice down to bedrock; concentrated flows (greater concentration of clasts) are more erosive than dilute flows (Scott, 1988; Major and Newhall, 1989; Pierson et al., 1990; Thouret, 1990; Walder, 1999; Barr et al., 2018). Attrition is particularly effective on steep and crevassed sections of glaciers and may cause beheading of glaciers. The commonest way in which lahars form on snow-capped volcanoes is by the transformation from flood surges produced by the interaction (transfer of heat) between pyroclasts in density currents, including block-and-ash flows, with snowpack or glacial ice (e.g. Scott, 1988; Trabant et al., 1994; Thouret, 1990; Pierson and Waitt, 1999). However, dilute pyroclastic currents (surges) probably generate less melt because they lack much thermal mass. Conversely, the more concentrated density currents (pyroclastic flows; block-and-ash flows) probably generate much more melt and entrain ice much more efficiently (Barr et al., 2018). This was demonstrated during the 1985 Nevado del Ruiz eruption in which the snow and ice surfaces over which the denser currents flowed were extensively melted, gouged and abraded (Pierson et al., 1990); flat-floored channels 2-4 m deep and up to 100 m wide were eroded into glacier ice.

By contrast, supraglacial accumulation of tephra by pyroclastic fall has a conflicting but probably minor impact on melting snow and ice. Within a narrow zone proximal to the vent, tephra deposits may have elevated temperatures (especially ballistic bombs, which melted holes up to 2 m in diameter and depth during the 1985 eruption of Nevado del Ruiz; Delgado Granados et al., 2021). Even larger melt pits are possible (see Fig. 26). Outside of

Figure 26. View of a small pyroclastic cone surrounded by snowpack showing numerous small melt pits caused by the ballistic impact and melting effects of large bombs. Using the diameter of the crater (c. 150 m) as a scale, the largest melt-pits seen in the view may be as much as 8 m in width. The cone is also flanked by a prominent moat probably created by radiant heat from the pyroclastic pile. More proximal snow (under the cone flank) was probably melted by the accumulation of tephra. Snow and moat are absent on the rear left flank of the cone as that flank collapsed during a prior episode of lava effusion. The dark-coloured terrain in the background is ash-covered ice. Mount Belinda, Montagu Island, South Sandwich Islands, 2006. Photograph by R. Ashurst.

that zone, tephra is probably cold when it lands. If the tephra layer is thin (< c. 2 cm), small debris flows may be triggered due in part to a reduced albedo, but they are unlikely to develop into significant meltwater floods. Moreover, because of the low thermal conductivity of tephra and its shielding properties, thicker layers of tephra protect underlying snow and ice thus reduce surface melting (Major and Newhall, 1989; Wilson et al., 2013; Barr et al., 2018; Manville et al., 2000; Edwards et al., 2020 and references therein).

Lava dome collapse by mechanical failure also transmits heat effectively by the penetration of snow by hot rock fragments. During dome growth, gravitational stresses acting on the brittle carapace can trigger mechanical failure accompanied by minor explosions from the ductile, gas-pressured dome core, with the failed mass moving away as a hot-rock avalanche that usually transforms into a block-and-ash flow (e.g. at Mt Redoubt in 1989 and 1990; Trabant et al., 1994; Pierson and Waitt, 1999a,b and references therein). By bringing hot rock into intimate contact with snow, the heat is transferred rapidly, triggering melting and resulting in large volumes of meltwater that, mixed with the hot volcanic debris, transform into lahars. Additional material is incorporated derived from older deposits, which rapidly increases the volume of the initial lahar, a process called bulking up. Bulking up, which is important in all lahars, is facilitated by the presence of easily erodible older deposits, such as poorly- or unconsolidated pyroclastic rocks, alluvium and a high topographical relief with steep slopes. Volume increases of 2-4 times during flow are not uncommon and the volume may increase by an order of magnitude (Pierson et al., 1990; Pierson and Waitt, 1999a).

In summary, whilst pyroclastic fall appears unable to melt significant quantities of snow outside of a vent-proximal zone, both low-concentration and high-concentration pdcs are the principal means by which a snow or ice substrate is thermally and mechanically eroded. Scouring and heat transfer from pdcs are more important than ice volume in many examples (Delgado Granados et al., 2021). However, because even small explosive eruptions deposit much hot debris close to a vent, both by fallout and as pdcs, the resulting focusing of hot rock/snowpack interactions in proximal locations is often particularly effective at generating meltwater.

Glaciovolcanic lahars also generate a distinctive hybrid type of mass flow called mixed avalanches or ice-slurries (Pierson and Janda, 1994; Waitt et al., 1994; Pierson et al., 1990; Lube et al., 2009; Waythomas et al., 2009). A prerequisite for their formation is the presence of extensive thick firn and snow. The deposits, called ice diamict, incorporate granular snow, blocks of ice and pyroclastic debris (pumice) in a matrix of sand ash and ice (frozen pore water); clasts of ice and snowpack may be as large as 2.5 m. Ice diamict can form composite deposits up to 20 m thick although individual beds are more typically 1-5 m thick. They are highly distinctive on deposition but the ice components and voids, which cumulatively may amount to as much as 80-90 % of the deposit by volume, soon collapse. The deposit deflates to a small fraction of its original thickness, thus removing the evidence for its unusual origin.

Finally, lava emplacement at low effusion rates (< 50 $m^3.s^{-1}$) creates water flows not lahars, and the volumes of melt are generally not large (Major and Newhall, 1989; Barr et al., 2018 and references therein; Edwards et al., 2012, 2016; Fig. 27). Small lahars are created at higher effusion rates whereas, at very high effusion rates (> 100 $m^3.s^{-1}$), accompanied by

lava fountaining, melting in the vent region can be sufficient to generate voluminous lahars (Delgado Granados et al., 2021).

Figure 27. View looking north at Big Ben, Heard Island, in 2016, showing several short lavas that flowed supraglacially before subsiding into the snowpack. Small meltwater floods evidently preceded each of the lavas, as evidenced by the discoloured snow streaks downslope of the lava-occupied channels. Despite the steep slopes, the lavas only flowed c. 400 m before terminating; the meltwater travelled at least a further 1200 m before vanishing into crevasses (below the cloud in the image). Photograph by P. Harmsen (CSIRO Marine National Facility, Australia).

The downflow transformation of floods follows a recognizable pattern (Fig. 28). Lahars begin as (melt)water flood surges, bulk up into debris flows, then debulk to transform into hyperconcentrated flows and, ultimately, streamflows (e.g. Pierson and Scott, 1985; Scott,
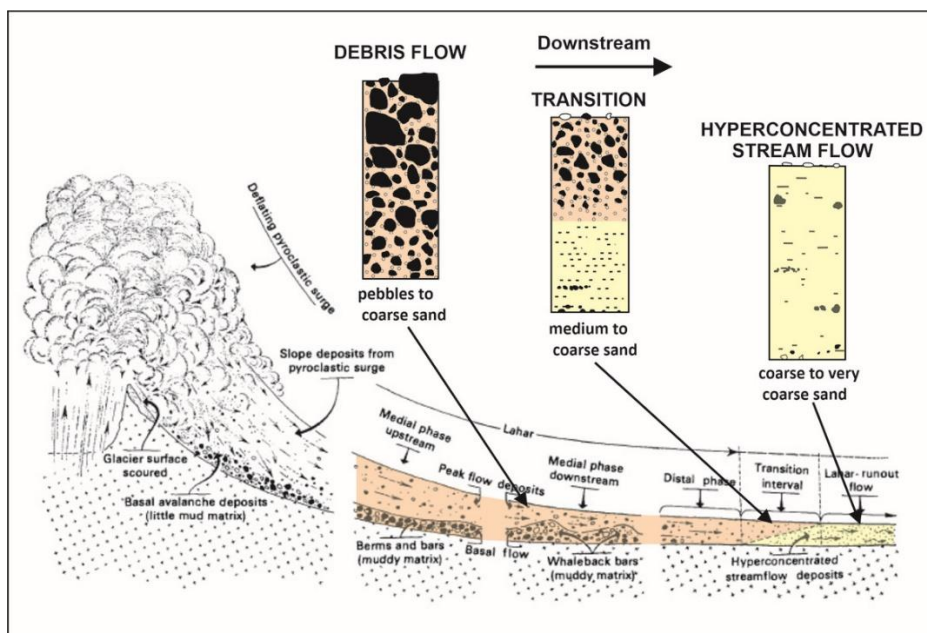
Figure 28. Sketch showing a lahar triggered by a supraglacial pyroclastic density current and its downflow transformation from debris flow to hyperconcentrated flow (from Scott, 1988; figure not subject to U.S. copyright). Also shown are schematic vertical profile sections through lithofacies representative of the flow conditions at different stages in the emplacement of the lahar (after Pierson and Scott, 1985; see also Scott, 1988). The mean grain sizes of each lithofacies are also indicated. Note how the debris flow lithofacies/stage

overrides the hyperconcentrated flow lithofacies/stage and terminates within a relatively short transition zone.

1988; Meyer and Trabant, 1995). Water surges unrelated to eruptions may take 20 km of more to transform to a debris flow, depending on how rapidly bulking up occurs (Scott, 1988). By contrast, clay-poor eruption-generated flood surges may transform much more rapidly; examples at Mount St Helens and Mount Rainier transformed from water floods to debris flows within 1 and 6.5 km, respectively (Pierson, 1999). A single lahar flood wave comprises a frontal portion that is hyperconcentrated (and becomes the lahar runout) and a tail that is a debris flow. The formation of hyperconcentrated flows is caused by the progressive incorporation of streamflow by the leading edge of the debris flow; the debris flow then overruns the hyperconcentrated flow in a short transition zone (Fig. 28) just prior to freezing. The rate of downstream transformation to a lahar runout is strongly influenced by the amount of clay in a lahar (Scott, 1988; Vallance and Scott, 1995). A higher proportion of clay (> 3-5 % by weight; measured values range up to 37 %) is typically present in nonvolcanic lahars derived by flank collapses incorporating hydrothermally-altered rock (Vallance and Scott, 1995; Delgado Granados et al., 2021). By contrast, eruption-derived lahars are generally more granular and less cohesive due to a lower proportion of clay (< 5 % by weight; Scott, 1988; Vallance and Iverson, 2015), which gives them a greater miscibility with overrun streamflow, and the hyperconcentrated flow stage probably has a greater lateral extent than those sourced in clay-rich lahars. Ultimately, the flows become so diluted by stream water that they become sediment-laden stream flows.

The progressive changes during flow are reflected in the sequence of lahar lithofacies deposited downstream (Fig. 28). Debris flow lithofacies are massive or weakly stratified, characterised by up to 80-90 % matrix (typically much less, down to < 10 %) composed of mainly sand-grade ash, pumice and lithic grains together with a very variable proportion of much larger lithic clasts, some of which may show radial cooling joints signifying that they were hot when incorporated. An extremely wide grain size is typical and clasts a few metres in diameter are not uncommon, with some exceeding 10 m (Fig. 29a,b; Mothes and Vallance, 2015; Procter et al., 2021). Most clasts are angular closer to source but the proportion of rounded clasts increases with distance and were picked up during bulking. Grading and sorting generally do not improve with distance from source, reflecting the high yield tendency of most debris flows in which the high matrix content prevents much mixing with water during flow, nor do the deposits fine markedly. Hyperconcentrated flow deposits are massive or faintly planar stratified with moderate to poor sorting (Fig. 29b,c). They are composed of sand or fine gravel with angular (mainly juvenile) to abraded clast shapes, the latter representing alluvial material picked up from stream beds during flow (Scott, 1988; Pierson, 2005; Procter et al., 2021). They may also show isolated lenses of gravel and pumice, an openwork texture with dispersed to imbricated outsize clasts up to boulder size, and dish and pillar structures indicative of dewatering (Fig. 29b,d). Lahars can be divided into a channel facies dominantly composed of the deposits of the basal debris flow, possibly with a sole layer ('traction carpet'; Scott, 1988; Thouret et al., 2020; Fig. 28); and a flood plain facies consisting of laterally extensive debris flows somewhat finer-grained than the channel facies, together with hyperconcentrated flow sheets. Ultimately the hyperconcentrated flows evolve into normal well-stratified streamflow (flood) deposits.

Figure 29. Compendium of photographs illustrating lahar lithofacies. A. Sandy breccio-conglomerate deposited by a debris flow, composed of variably angular to abraded cobles and boulders set in fine sand matrix with scattered pumice clasts; the ice axe is 70 cm long. B. Debris flow deposit (sandy breccio-conglomerate) overlying a hyperconcentrated flow deposit; the latter is medium to coarse sandstone with faint planar laminations, a few fine gravel lenses and dispersed outsize clasts. C. Close view of hyperconcentrated flow deposit shown in (B); note faint planar lamination and washout structure; the ice axe head is 30 cm long. D. Prominent dish and pillar structures in a hyperconcentrated flow deposit, caused by dewatering. All photographs of ravine-filling deposits on Mason Spur volcano (Late Miocene), Antarctica. It is not certain that the volcano was ice-capped but the lithofacies are representative of lahar deposits generally.

Discussion and conclusions

Despite the widespread occurrence of glacierized landscapes and glaciovolcanism on Earth, past and present, there is no comprehensive discussion of the range of sedimentary deposits associated with the volcanism and only the proglacial deposits are well studied. Three discrete groups of deposits are recognized: englacial cavity, jökulhlaup and lahar.

Englacial cavity deposits are identified here as an important yet little recognised sedimentary association linked directly to glaciovolcanism. They are probably only associated with small monogenetic glaciovolcanoes or groups of monogenetic volcanoes associated with a longer-lived eruptive fissure. Very few examples are known and all are in Iceland (Bennett et al., 2006, 2009). It is possible that they have been overlooked but it is also likely that special circumstances are required for their development, specifically an ice sheet coeval with the glaciovolcanism that is moving sufficiently rapidly that an englacial cavity is opened up. A cavity will open up if the rate of ice melting during flow around a volcano exceeds the rate of cavity closure due to normal cryostatic pressure (Smellie and Panter, 2021). Englacial cavity deposits can form in somewhat different situations depending on whether the glaciovolcano is active or the location is simply experiencing enhanced geothermal activity but not an eruption (Fig. 30). In the former case, the ice roof

will be removed over the lee-side englacial cavity if the eruption becomes subaerial (true for
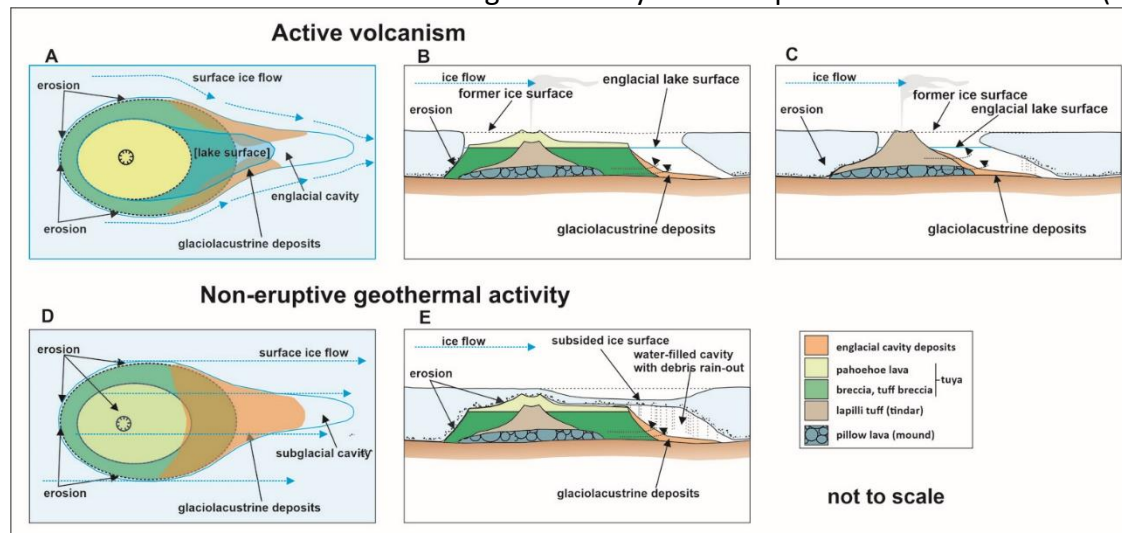
Figure 30. Schematic plan views and cross sections illustrating different situations capable of generating lee-side englacial cavities with associated glaciolacustrine deposits. A-C: Active glaciovolcano has melted completely through an ice sheet. The deposits contain an abundance of juvenile clasts, and dropstones are uncommon except in marginal locations. The cavity will generally be significantly larger for tuyas (B), with their laterally spreading lava-fed deltas, compared with tuff cones or tindars (C). There is currently no known example of deposition associated with an active tuya but a possible depositional setting for outcrops at Jarlhettur is depicted by C. D-E: Situation envisaged for areas of active geothermal activity not resulting in a volcanic eruption (cf. Bennett et al., 2006, fig. 11a), a situation that may have prevailed in the Laugarvatn area, with deposits characterised by polymict abraded debris and abundant dropstones discharged from an actively overriding ice roof. Although an active glaciovolcanic pillow mound will also not melt through the ice roof, it is unclear whether the very low profile of the mound and the relatively slow meltwater generation (melting by conduction and convection) are capable of generating a substantial lee-side cavity. No examples are currently known.

tuya and most tindar glaciovolcanoes), but it typically remains in place in situations involving only geothermal activity. The differences should result in detectable variations in the resulting deposits, especially in the presence and abundance of dropstones (ice roof present; geothermally heated edifice) or their scarcity (ice roof absent; coeval volcanic eruption), and in the dominant clast type (polymict or monomict, respectively). In cases where a glaciovolcano ceases activity without melting through its ice roof, which is probably true for most glaciovolcanic pillow mounds, there may be no distinction. However, it is currently unclear whether the low profiles of pillow mounds, which generate meltwater only slowly (Gudmundsson, 2003), are capable of generating substantial lee-side englacial cavities. No examples associated with pillow mounds have yet been described.

Englacial cavity deposits in the Laugarvatn area appear to be polymict, with abraded clast shapes, and no clearly identified juvenile material (Bennett et al., 2006). Dropstones are abundant throughout. Moreover, at Laugarvatn the volcanic centres associated with englacial cavity deposits are tuyas and tuya construction involves the lateral progradation of lava-fed deltas. The associated ice is melted through completely above the volcanic edifice. In the absence of an ice roof over the cavity, dropstones (representing released glacial bedload) are unlikely to form except possibly to limited effect in marginal locations (Fig. 30a,b). Thus, the presence of abundant dropstones in the Laugarvatn sequences (Fig. 11) probably implies that an ice roof was formerly present and the ice cavity was probably

heated during an episode of enhanced geothermal flux rather than with a recently erupting (unconsolidated) glaciovolcano.

By contrast, analogous deposits at Jarlhettur are generally rich in angular juvenile detritus (lapilli—ash hyaloclasts), apart from in a basal polymict layer in which dropstones are also locally common (Bennett et al. (2009). The deposits are thus mainly linked to erosion of unconsolidated tephras in the associated tindar and they were also deformed by the edifice as it grew and expanded. Although the contemporaneous ice sheet was melted through, the area of ice removed by an explosively generated conical edifice would be much smaller than during tuya development. Figure 30c shows a possible reconstruction of the depositional setting at Jarlhettur, with sediment fans growing inward from the sides of an englacial vault. Bennett et al. (2009) also suggested that inflow of meltwater to the fan sites might be enhanced by reconfiguring of the pre-existing glacial drainage network to focus on the eruptive site(s) due to effects on the hydraulic potentials caused by the geothermal anomaly (cf. Björnsson, 1988). Such focussing would increase the volume of basal sediment delivered to the vault.

The lateral extent of the fan-like englacial cavity deposits is substantial, variably ≥ 1.2-3.5 km at Laugarvatn and at least 0.75 km at Brekknafjöll—Jarlhettur. The distances correspond to minimum extents of the associated englacial vaults, and the three-dimensional morphology is not yet well defined due to glacial removal of many deposits. The presence of large channel bedforms in the deposits was linked by Bennett et al. (2006) to possible jökulhlaup events, but how strong currents could also occur between such events, to explain the smaller channels, was regarded as inexplicable. However, a leaky vault is likely to generate a strong continuous but fluctuating flux of escaping (warm) meltwater (Smellie, 2006) and sudden jökulhlaup events need not always be necessary to create water flow and channels. The observation of axially focussed currents described by Bennett et al. (2006) suggests tunnel flow, with currents deflected centroclinally by the tunnel margins (also possibly seen at Arnarþúfur; cf. Hamilton, 2004), but other interpretations are possible. It is unclear how representative the fan dimensions are but it may be significant that the most extensive vaults appear to be associated with fans in the Laugarvatn area. Perhaps the duration of high geothermal heat flow associated with the Laugarvatn fans (lacking coeval volcanism?) was much longer than that associated with fans at Brekknafjöll—Jarlhettur (associated with a relatively short-lived pulse of volcanism?), thus permitting a longer period of melting of overlying ice and deposition of larger sediment volumes. Further examples need to be described to test this suggestion.

This study has also highlighted, for the first time, that distinctive glaciovolcanic units known as sheet-like sequences (Smellie, 2008; Smellie and Edwards, 2016) are the proximal, subglacial equivalents of subaerial (sandar) jökulhlaup deposits (Fig. 31). The sheet-like sequences represent an important opportunity to examine the processes involved in jökulhlaup development, and for understanding sediment transport paths and volumes, in an ultra-proximal location that is wholly inaccessible to view during modern jökulhlaup events. Examples of sheet-like sequences and jökulhlaup deposits are widespread in Iceland but they are rare elsewhere. A challenge also exists reconciling the terminology used for sheet-like sequences and jökulhlaup deposits, with volcanic terminology used for the former but epiclastic terminology for the latter, despite both being linked to the same event(s).
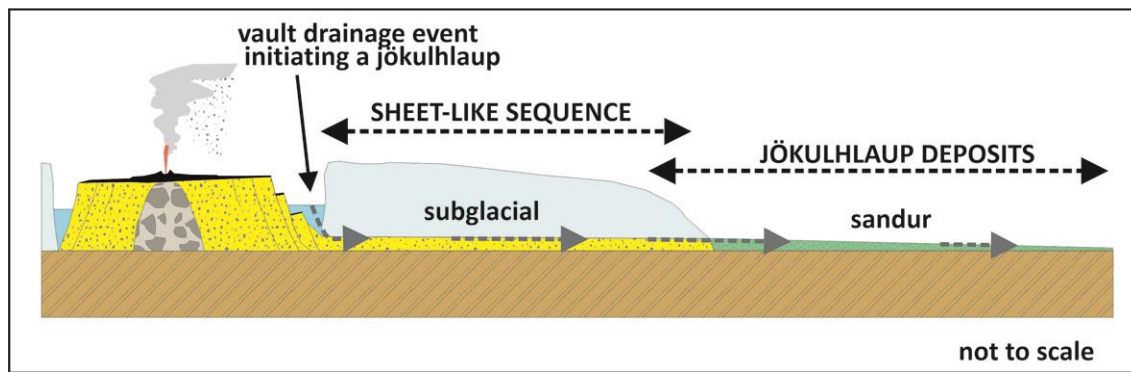
Figure 31. Schematic diagram illustrating the emplacement of sheet-like sequences and jökulhlaup deposits, which are proximal (ice-covered) and distal (subaerial) equivalents, respectively, deposited during the same volcanogenic outburst-flood event(s). Sheet-like sequence interface sill (Smellie, 2008) not shown, for clarity. Although the sketch depicts features associated with a large monogenetic tuya, similar processes occur on the flanks and proglacial sandar of large polygenetic glaciovolcanoes.

Despite different triggering conditions, in many respects the products of jökulhlaups and lahars are identical (i.e. debris flow and hyperconcentrated flow deposits) and show the same transitions downflow. However, debris flow deposits require steep gradients to maintain flow and they appear to be volumetrically much commoner in the lahar settings associated with stratovolcanoes, with their typically steep flanks (Fig. 28). They are generally minor in volcanogenic jökulhlaup sequences, in which they are mainly preserved close to the ice terminus (Maizels, 1997). They are also a minor lithofacies within sheet-like sequences, although examples containing sandy matrix-rich conglomerate and pebbly mudstone are sometimes present (Bergh, 1985; Smellie et al., 1993). However, the flows that created sheet-like deposits are usually clay-poor and dominated by coarse ash- and lapilli-size juvenile glass clasts, which enables them to transform to hyperconcentrated flows rapidly. Debris flows are much more prominent in jökulhlaups that are channel-confined (Carrivick et al., 2004b). Mixed-avalanche or ice-slurry flows (and their ice diamict deposits) appear to be unique to lahars, as are lahars generated by dome collapses. Ice diamicts have no significant preservation potential. Lahars linked to dome collapse are distinctive in being dominated by poorly or non-vesicular, monomict, aphanitic juvenile clasts. Further differences between lahars and jökulhlaups include the following: (1) Lahar events are generally shorter in duration, reflecting the generally much greater volume of water stored subglacially that is released suddenly in jökulhlaups. (2) Lahar hydrographs may more frequently show multiple peaks that attenuate downstream but there is clear overlap in this characteristic. (3) Lahars are triggered within minutes of an eruption but jökulhlaups may lag the eruption initiation by several days to a few weeks. (4) Studies of lahars show a much stronger focus on channel flow and channel deposits (dominated by debris flows) because most examples include a prominent valley-confined section; by contrast, low-gradient flood plains (sandur) are the principal focus of jökulhlaups studies, probably because the source regions are currently still covered by ice and thus inaccessible.

In glaciovolcanic eruptions beneath thick ice (> 200 m) that are characterized mainly by finely particulate tephra cones and ridges formed by explosive hydrovolcanic eruptions, the efficiency of ice melting is much greater than during eruptions distinguished by lava effusion and much slower conductive cooling (70-80 % efficiency versus 10-45 %, respectively; Gudmundsson, 2003). Thus, explosive glaciovolcanic eruptions associated with thick ice shall generate abundant meltwater much more rapidly, quickly filling the englacial vault and

enhancing the likelihood of relatively early jökulhlaups compared with effusive eruptions. The implications for volcanic risk assessment are obvious. Moreover, the timing of flooding in relation to eruption initiation is inversely proportional to ice thickness (smaller vaults (thinner ice) shall fill and discharge more rapidly than larger vaults (thicker ice)). The eruption of Eyjafjallajökull in 2010, with c. 200 m-thick ice in its summit caldera, released meltwater rapidly in jökulhlaups. It is an example of a volcano at the transition between ice-covered (i.e. ≥ c. 200 m thick) and ice-capped (thinner ice). If ice thinning continues due to climate change, the volcano shall become associated with lahars rather than jökulhlaups.

These observations affect glaciovolcanic eruptions under wet-based ice. By contrast, meltwater generated during a volcanic eruption under cold-based ice is sealed into the vault by the surrounding ice, the ice cannot be floated and the meltwater can only escape supraglacially. Thus, basal debris is never accessed at any stage during flooding. However, the resulting supraglacial jökulhlaups will entrain large quantities of coeval tephra deposited on the surrounding ice surface. This might result in the construction of ice-proximal, supraglacially-sourced outwash fans of *hochsandur* type, which are relatively small features (Krüger, 1997; Kjær et al., 2004). With their distinctive sedimentary characteristics and lack of proximal to distal transitions, glaciovolcanic *hochsandur* deposits should be recognizable in the geological record.

Finally, it is worth noting that, despite being surrounded by the Antarctic Ice Sheet (the largest ice sheet on Earth), many Antarctic volcanoes have a relatively thin cover of ice over their summits except where they contain a caldera filled by thicker ice. They are also mainly associated with cold-based ice unlike glaciovolcanoes at mid and lower latitudes, and the implications for sedimentation coeval with eruptions in Antarctica are not certain. As indicated above, jökulhlaups are unlikely since the ice is frozen to its bed. Moreover, any lahars that are generated will be deposited supraglacially and advected to the sea by ice flow, where they shall probably be unrecognizable in the geological record.

Acknowledgements

References

Alho, P., Russell, A.J., Carrivick, J.L. and Käyhko, J. 2005. Reconstruction of the largest Holocene jökulhlaup within Jökulsa á Fjöllum, NE Iceland. Quaternary Science Reviews, 24, 2319-2334.

Baker, V.R., Benito, G. and Rudoy, A.N. 1993. Palaeohydrology of late Pleistocene superflooding, Altay Mountains, Siberia. Science, 259, 348–350.

Banik, T.J., Wallace, P.J., Höskuldsson, Á., Miller, C.F., Bacon, C.R. and Furbish, D.J. 2014. Magma—ice—sediment interactions and origin of lava/hyaloclastite sequences in the Síða formation, South Iceland. Bulletin of Volcanology, 76:785, doi:10.1007/s00445-013-0785-3.

Barr, I.D., Lynch, C.M., Mullan, D., De Siena, L. and Spagnolo, M. 2018. Volcanic impacts on modern glaciers: A global synthesis. Earth-Science Reviews, 182, 186-203.

Bennett, M.R., Huddart, D. and Waller, R.I., 2006. Diamict fans in subglacial water-filled cavities—a new glacial environment. Quaternary Science Reviews, 25, 3050–3069.

Bennett, M.R., Huddart, D. and Gonzalez, S. 2009. Glaciovolcanic landsystems and large-0scale glaciotectonic deformation along the Brekknafjöll—Jarlhettur, Iceland. Quaternary Science Reviews, 28, 647-676.

Bergh, S. 1985. Structure, depositional environment and mode of emplacement of basaltic hyaloclastites and related lavas and sedimentary rocks: Plio-Pleistocene of the eastern volcanic rift zone, southern Iceland. Nordic Volcanological Institute Report, No. 8502, 91 pp.

Bergh, S. and Sigvaldason, G.E. 1991. Pleistocene mass-flow deposits of basaltic hyaloclastite on a shallow submarine shelf, South Iceland. Bulletin of Volcanology, 53, 597-611.

Björnsson, H. 1988. Hydrology of icecaps in volcanic regions. Vísindafélag Íslendinga, Societas Scientarium Islandica, 45, 1-139.

Björnsson, H. 1992. Jökulhlaups in Iceland: prediction, characteristics and simulation. Annals of Glaciology, 16, 95-106.

Björnsson, H. 1998. Hydrological characteristics of the drainage system beneath a surging glacier. Nature, 395, 771-774.

Björnsson, H. 2002. Subglacial lakes and jökulhlaups in Iceland. Global and Planetary Change, 35, 255-271.

Björnsson, H., Pálsson, F. and Gudmundsson, M.T. 2000. Surface and bedrock topography of the Mýrdalsjökull ice cap, Iceland: The Katla caldera, eruption sites and routes of jökulhlaups. Jökull, 49, 29-46.

Branney, M.J. and Gilbert, J.S. 1995. Ice-melt collapse pits and associated features in the 1991 lahar deposits of Volcán Hudson, southern Chile: criteria to distinguish eruption-induced glacier melt. Bulletin of Volcanology, 57, 293–302.

Branney, M.J. and Kokelaar, P. 2002. Pyroclastic density currents and the sedimentation of ignimbrites. Geological Society, London, Memoir, 27, 143 pp.

Brown, R.J., Bonadonna, C. and Durant, A.J. 2012. A review of ash aggregation. Physics and Chemistry of the Earth, 45-46, 65-78.

Carr, M.H. and Head, J.W. 2010. Geologic history of Mars. Earth and Planetary Science Letters, 294, 185-203.

Carrivick, J.L. 2007. Hydrodynamics and geomorphic work of jökulhlaups (glacial outburst floods) from Kverkfjöll volcano, Iceland. Hydrological Processes, 21, 725-740.

Carrivick, J.L., Russell, A.J. and Tweed, F.S. 2004a. Geomorphological evidence for jökulhlaups from Kverkfjöll volcano, Iceland. Geomorphology, 63, 81-102.

Carrivick, J.L., Russell, A.J., Tweed, F.S. and Twigg, D. 2004b. Palaeohydrology and sedimentary impacts of jökulhlaups from Kverkfjöll, Iceland. Sedimentary Geology, 172, 19-40.

Carrivick, J.L., Pringle, J.K., Russell, A.J. and Cassidy, N.J. 2007. GPR-derived sedimentary architecture and stratigraphy of outburst flood sedimentation within a bedrock valley system, Hraundalur, Iceland. Journal of Environmental and Engineering Geophysics, 12, 127-143.

Carrivick, J.L. and Tweed, F.S. 2019. A review of glacier outburst floods in Iceland and Greenland with a megafloods perspective. Earth-Science Reviews, 196, 102876, doi.org/10.1016/j.earscirev.2019.102876

Chapman, M.G., Allen, C.C., Gudmundsson, M.T., Gulick, V.C., Jakobsson, S.P., Lucchitta, B.K., Skilling, I.P. and Waitt, R.B. 2000. Volcanism and ice interactions on Earth and Mars. In: Zimbelman, J.R. and Gregg, T.K.P. (eds) Environmental effects on volcanic eruptions. Kluwer Academic/Plenum Publishers, New York, pp. 39-74.

Cole, R.P., White, J.D.L., Conway, C.E., Leonard, G.S., Townsend, D.B. and Pure, L.R. 2018. The glaciovolcanic evolution of an andesitic edifice, South Crater, Tongariro, New Zealand. Journal of Volcanology and Geothermal Research, 352, 55-77.

Conway, C.E., Townsend, D.B., Leonard, G.S., Wilson, C.J.N., Calvert, A.T. and Gamble, J.A. 2015. Lava-ice interaction on a large composite volcano: a case study from Ruapehu, New Zealand. Bulletin of Volcanology, 77, 21, doi:10.1007/s00445-015-0906-2

Curtis A. and Kyle, P. 2017. Methods for mapping and monitoring global glaciovolcanism. Journal of Volcanology and Geothermal Research, 333-334, 134-144.

Delgado Granados, H., Miranda, P.J., Carrasco Núñez, G., Alzate, B.P., Mothes, P., Moreno Roa, H., Cáceres Correa, B.E. and Cortés Ramos, J. 2021. Hazards at ice-clad volcanoes: Phenomena, processes, and

examples from Mexico, Colombia, Ecuador, and Chile. In: Haeberli, W. and Whiteman, C. (eds) Snow and ice-related hazards, risks, and disasters. Elsevier, Amsterdam, Netherlands, pp. 597-639.

Donoghue, S.L. and Neall, V.E. 2001. Late Quaternary constructional history of the southeastern Ruapehu ring plain, New Zealand. New Zealand Journal of Geology and Geophysics, 44, 439-466.

Duller, R.A., Mountney, N.P., Russell, A.J. and Cassidy, N.C. 2008. Architectural analysis of a volcaniclastic jökulhlaup deposit, southern Iceland: sedimentary evidence for supercritical flow. Sedimentology, 55, 939-964.

Duller, R.A., Warner, N.H., McGonigle, C., De Angelis, S., Russell, A.J. and Mountney, N.P. 2014. Landscape reaction, response, and recovery following the catastrophic 1918 Katla jökulhlaup, southern Iceland. Geophysical Research Letters, 41, 4214-4221.

Dunning, S.A., Large, A.R.G., Russell, A.J., Roberts, M.J., Duller, R., Woodard, J., Mériaux, A.-S., Tweed, F.S. and Lim, M. 2013. The role of multiple glacier outburst floods in proglacial landscape evolution: The 2010 Eyjafjallajökull eruption, Iceland. Geology, 41, 1123-1126.

Edwards, B., Magnússon, E., Thordarson, T., Gudmundsson, M.T., Höskuldsson, A., Oddsson, B. and Haklar, J. 2012. Interactions between lava and snow/ice during the 2010 Fimmvörðuháls eruption, south-central Iceland. Journal of Geophysical Research, 117, B04302, doi:10.1029/2011JB008985

Edwards, B.R., Belousov, A., Belousova, M. and Melnikov, D. 2016. Observations on lava, snowpack and their interactions during the 2012-13 Tolbachik eruption, Klyuchevskoy Group, Kamchatka Peninsula, Russia. Journal of Volcanology and Geothermal Research, 307, 107-119.

Edwards, B.R., Russell, J.K., Gudmundsson, M.T. 2015. Glaciovolcanism. In: Sigurdsson, H., Houghton, B., Rymer, H., Stix, J. and McNutt, S. (eds) The Encyclopedia of Volcanoes, 2nd Edition. Academic Press, San Diego, pp. 377–393.

Edwards, B., Kochtitsky, W and Battersby, S. 2020. Global mapping of future volcanism. Global and Planetary Change, 195, 103356, doi.org/10.1016/j.gloplacha.2020.103356

Einarsson, B., Jóhannesson, T., Thorsteinsson, T., Gaidos, E. and Zwinger, T. 2017. Subglacial flood path development during a rapidly rising jökulhlaup from the western Skaftá cauldron, Vatnajökull, Iceland. Journal of Glaciology, 240, 670-682.

Elíasson, J. 2008. A glacial burst tsunami near Vestmannaeyjar, Iceland. Journal of Coastal Research, 24, 13–20.

Elíasson, J., Larsen, G., Guðmundsson, M.T. and Sigmundsson, F. 2006. Probabilistic model for eruptions an associated flood events in the Katla caldera, Iceland. Computational Geosciences, 10, 179-200.

Elíasson, J., Kjaran, S.P., Holm, S.L., Guðmundsson, M.T and Larsen, G. 2007. Large hazardous floods as translatory waves. Environmental Modelling and Software, 22, 1392–1399.

Everest, J. and Bradwell, T. 2003. Buried glacier ice in southern Iceland and its wider significance. Geomorphology, 52, 347–358.

Fassett, C.I. and Head, J.W. 2006. Valleys on Hecates Tholus, Mars: origin by basal melting of summit snowpack. Planetary and Space Science, 54, 370-378.

Fassett, C.I. and Head, J.W. 2007. Valley formation on martian volcanoes in the Hesperian: Evidence for melting of summit snowpack, Caldera lake formation, drainage and erosion of Ceraunius Tholus. Icarus, 189, 118-135.

Fay, H. 2002a. Formation of kettle holes following a glacial outburst flood (jökulhlaup), Skeiðarársandur, southern Iceland. International Association of Hydrological Sciences Publication, 271, 205-210.

Fay, H. 2002b. Formation of ice-block obstacle marks during the November 1996 glacier-outburst flood (jökulhlaup), Skeiðarársandur, southern Iceland. Special Publication of the International Association of Sedimentologists, 32, 85-97.

Fisher, R.V. and Smith, G.A. (eds) 1991. Sedimentation in volcanic settings. SEPM Special Publication, 45, 257 pp.

Forbes, A.E.S., Blake, S. and Tuffen, H. 2014. Entablature: fracture type and mechanisms. Bulletin of Volcanology, 76, 820, doi:10.1007/s00445-014-0820-z

Fountain, A.G. and Walder, J.S. 1998. Water flow through temperate glaciers. Reviews of Geophysics, 36, 299-328.

Friele, P.A., Clague, J.J., Simpson, K. and Stasiuk, M. 2005. Impact of a Quaternary volcano on Holocene sedimentation in Lillooet River valley, British Columbia. Sedimentary Geology, 176, 305-322.

Friele, P., Jakob, M. and Clague, J. 2008. Hazard and risk from large landslides from Mount Meager volcano, British Columbia, Canada. Georisk, 2, 48-64.

Glen, J.W. 1954. The stability of ice-dammed lakes and other water-filled holes in glaciers. Journal of Glaciology, 2, 316-318.

Gomez, B., Smith, L.C., Magilligan, F.J., Mertes, L.A. and Smith, N.D. 2000. Glacier outburst floods and outwash plain development, Skeiðarársandur, Iceland. Terra Nova, 12, 126-318.

Gudmundsson, M.T. 2003. Melting of ice by magma-ice-water interactions during subglacial eruptions as an indicator of heat transfer in subaqueous eruptions. In: White, J.D.L., Smellie, J.L. and Clague, D.A. (eds) Subaqueous explosive volcanism. American Geophysical Union, Geophysical Monograph Series, 140, pp. 61-72.

Gudmundsson, M.T., 2015. Hazards from Lahars and Jökulhlaups. In: Sigurdsson, H., Houghton, B., Rymer, H., Stix, J. and McNutt, S. (eds) The Encyclopedia of Volcanoes, 2nd Edition. Academic Press, San Diego, pp. 971–984.

Gudmundsson, M.T., Sigmundsson, F. and Björnsson, H. 1997. Ice—volcano interaction in the 1996 Gjálp eruption, Vatnajökull, Iceland. Nature, 389, 954-957.

Gudmundsson, M.T., Högndóttir, Th., Kristinsson, A.B. and Gudbjörnsson, S. 2007. Geothermal activity in the subglacial Katla caldera, Iceland, 1999-2005, studied with radar altimetry. Annals of Glaciology, 45, pp. 66-72.

Gudmundsson, M.T., Thordarson, T., Höskuldsson, Á., Larsen G., Björnsson, H., Prata, A.J., Oddsson, B., Magnússon, E., Högnadóttir, T., Pedersen, G.N., Hayward, C.L., Stevenson, J.A. and Jónsdóttir, I. 2012. Ash generation and distribution from the April-May 2010 eruption of Eyjafjallajökull, Iceland. Nature Scientific Reports, 2, 572, doi:10.1038/srep00572

Hackett, W.R. and Houghton, B.F. 1989. A facies model for a Quaternary andesitic composite volcano: Ruapehu, New Zealand. Bulletin of Volcanology, 51, 51-68.

Hambrey, M.J. and Glasser, N.F. 2005. Sedimentary processes – glaciers. In: Selley, R.C., Cocks, R.M. and Plimer, I.R. (eds) Encyclopedia of geology. Elsevier, pp. 663-678.

Hamilton, C.W. 2004. Ice-contact volcanism in the Vífilsfell region, southwest Iceland. BSc thesis, Dalhousie University, USA, 190 p. [unpubl.]

Harrison, D., Ross, N., Russell, A.J. and Dunning, S.A. 2019. Post-jökulhlaup geomorphic evolution of the Gígjökull Basin, Iceland. Annals of Glaciology, 60, 127-137.

Hubbard, A., Sugden, D., Dugmore, A., Norddahl, H. and Pétursson, H.G. 2006. A modelling insight into the Icelandic Last Glacial Maximum ice sheet. Quaternary Science Reviews, 2283-2296.

Hubbard, B., Souness, C. and Brough, S. 2014. Glacier-like forms on Mars. The Cryosphere, 8, 2047-2061.

Huggel, C., Ceballos, J.L., Pulgarín, B., Ramírez, J. and Thouret, J.-C. 2007. Review and reassessment of hazards owing to volcano—glacier interactions in Colombia. Annals of Glaciology, 45, 128-136.

Jóhannesson, T. 2002. The initiation of the 1996 jökulhlaup from Lake Grímsvötn, Vatnajökull, Iceland. International Association of Hydrological Sciences Publication, 271, 57-64.

Jones, J.J. 1969. Intraglacial volcanoes of the Laugarvatn region, south-west Iceland-I. Quarterly Journal of the Geological Society of London, 124, 197–211.

Jones, J.J. 1970. Intraglacial volcanoes of the Laugarvatn region, Southwest Iceland, II. Journal of Geology, 78, 127–140.

Jónsson, J. 1982. Notes on the Katla volcanogenic debris flows. Jökull, 32, 61–68.

Kelman, M.C., Russell, J.K. and Hickson, C.J. 2002. Effusive intermediate glaciovolcanism in the Garibaldi Volcanic Belt, southwestern British Columbia, Canada. Geological Society, London, Special Publications, 202, 195-211.

Kjær, K.H., Sultan, L., Krüger, J. and Schomacker, A. 2004. Architecture and sedimentation of outwash fans in front of the Mýrdalsjökull ice cap, Iceland. Sedimentary Geology, 172, 139-163.

Kjartansson, G. 1951. Water flood and mudflows. In: Einarsson, T. Kjartansson, G. and Thorarinsson, S. (eds) The eruption of Hekla 1947-48. Visindafelag Islendinga (Soc Sci Islandica) Reykjavik II, 4, 1-51.

Komatsu, G., Arzhannikov, S.G., Arzhannikova, A.V. and Ershov, K. 2007a. Geomorphology of subglacial volcanoes in the Azas Plateau, the Tuva Republic, Russia. Geomorphology, 88, 312-328.

Komatsu, G., Arzhannikov, S.G., Arzhannikova, A.V. and Ori, G.G. 2007b. Origin of glacial—fluvial landforms in the Azas Plateau volcanic field, the Tuva Republic, Russia: Role of ice—magma interaction. Geomorphology, 88, 352-366.

Krüger, J. 1997. Development of minor outwash fans at Kötlujökull, Iceland. Quaternary Science Reviews, 16, 649-659.

Larsen, G. 2000. Holocene eruptions within the Katla volcanic system, south Iceland: Characteristics and environmental impact. Jökull, 49, 1-28.

Loughlin, S.C. 2002. Facies analysis of proximal subglacial and proglacial volcaniclastic successions at the Eyafjallajökull central volcano, southern Iceland. Geological Society, London, Special Publication, 202, 149–178.

Lowe, D.R., Williams, S.N., Leigh, H., Connor, C.B., Gemmell, J.B. and Stoiber, R.E. 1986. Lahars initiated by the 13 November 1985 eruption of Nevado del Ruiz, Colombia. Nature, 324, 1-53.

Lube, G., Cronin, S.J. and Procter, J.N. 2009. Explaining the extreme mobility of volcanic ice-slurry flows, Ruapehu volcano, New Zealand. Geology, 37, 15-18.

Magnússon, E., Gudmundsson, M.T., Roberts, M.J., Sigurðsson, G., Höskuldsson, F. and Oddsson, B. 2012. Ice-volcano interactions during the 2010 Eyjafjallajökull eruption, as revealed by airborne imaging radar. Journal of Geophysical Research, 117, B07405, doi:10.1029.2012JB009250

Magnússon, E., Pálsson, F., Björnsson, H. and Gudmundsson, S. 2013. Removing the ice cap of Öræfajökull central volcano, SE-Iceland: Mapping and interpretation of bedrock topography, ice volumes, subglacial troughs and implications for hazards assessments. Jökull, 62, 131-150.

Major, J.J. and Newhall, C.G. 1989. Snow and ice perturbation during historical volcanic eruptions and the formation of lahars and floods - a global review. Bulletin of Volcanology, 52, 1-27.

Maizels, J. 1989. Sedimentology, paleoflow dynamics and flood history of jökulhlaup deposits: paleohydrology of Holocene sediment sequences in southern Iceland sandur deposits. Journal of Sedimentary Petrology, 59, 204-223.

Maizels, J.K. 1992. Boulder ring structures produced during jökulhlaup flows – origin and hydraulic significance. Geografiska Annaler, 74A, 21–33.

Maizels, J.K. 1993. Lithofacies variations within sandur deposits: the role of runoff regime, flow dynamics and sediment supply characteristics. Sedimentary Geology, 85, 299-325.

Maizels, J. 1997. Jökulhlaup deposits in proglacial areas. Quaternary Science Reviews, 16, 793-819.

Manville, V., Hodgson, K.A., Houghton, B.F. and White, J.D.L. 2000. Tephra, snow and water: complex sedimentary responses at an active snow-capped stratovolcano, Ruapehu, New Zealand. Bulletin of Volcanology, 62, 278–293.

Marren, P.M., Russell, A.J. and Rushmer, E.L. 2009. Sedimentology of a sandur formed by multiple jökulhlaups, Kverkfjöll, Iceland. Sedimentary Geology, 213, 77-88.

McGarvie, D. 2009. Rhyolitic volcano—ice interactions in Iceland. Journal of Volcanology and Geothermal Research, 185, 367-389.

McGarvie, D.W., Stevenson, J.A., Burgess, T., Tuffen, H. and Tindle, A.G. 2007. Volcano—ice interactions at Prestahnúkur, Iceland: rhyolite eruption during the last interglacial—glacial transition. Annals of Glaciology, 45, pp. 38-47.

McPhie, J., Doyle, M., and Allen, R. 1993. Volcanic textures: A guide to the interpretation of textures in volcanic rocks: Hobart, CODES Key Centre, University of Tasmania, 196 pp.

Mellors, R.A., Waitt, R.B. and Swanson, D.A. 1988. Generation of pyroclastic flows and surges by hot-rock avalanches from the dome of Mount St. Helens volcano, USA. Bulletin of Volcanology, 50, 14-25.

Meyer, D.F. and Trabant, D.C. 1995. Lahars from the 1992 eruptions of Crater Peak, Mount Spurr volcano, Alaska. United States Geological Survey Bulletin, 2139, 183-198.

Mothes, P.A., Hall, M.L. and Janda, R.J. 1998. The enormous Chillos Valley lahar: an ash-flow-generated debris flow from Cotopaxi volcano, Ecuador. Bulletin of Volcanology, 59, 233-244.

Mothes, P.A. and Vallance, J.W. 2015. Lahars at Cotopaxi and Tungurahau volcanoes, Ecuador: Highlights from stratigraphy and observational records and related downstream hazards. In: Shroder, J.F. and Papale, P. (eds) Volcanic hazards, risks and disasters. Elsevier, Amsterdam, Netherlands, pp. 141-168.

Naranjo, J.A. and Stern, C.R. 1998. Holocene explosive activity of Hudson Volcano, southern Andes. Bulletin of Volcanology, 59, 291-306.

Olszewski, A. and Weckwerth, P. 1999. The morphogenesis of kettles in the Höfjabrekkujökull forefield, Mýrdalssandur, Iceland. Jökull 47,71–88.

Pagneux, E., Gudmundsson, M.T., Karlsdóttir, S. and Roberts, M.J. (eds) 2015. Volcanogenic floods in Iceland. An assessment of hazards and risks at Öræfajökull and on the Markarfljót plain. Rekjavik: IMO, IES-UI, NCIP-DCPEM, 164 pp.

Palmer, B.A., Purves, A.M. and Donoghue, S.L. 1993. Controls on accumulation of a volcaniclastic fan, Ruapehu composite volcano, New Zealand. Bulletin of Volcanology, 55, 176-189.

Pierson, T.C. 1985. Initiation and flow behavior of the 1980 Pine Creek and Muddy River lahars, Mount St. Helens, Washington. Geological Society of America Bulletin, 96, 1056-1069.

Pierson, T.C. 1995. Flow characteristics of large eruption-triggered debris flows at snow-clad volcanoes: constraints for debris-flow models. Journal of Volcanology and Geothermal Research, 66, 283-294.

Pierson, T.C. 1999. Transformation of water flood to debris flow following the eruption-triggered transient-lake breakout from the crater on March 19, 1982. United States Geological Survey Professional Paper, 1586, 19-36.

Pierson, T.C. 2005. Hyperconcentrated flow - transitional process between water flow and debris flow. In: Jakob, M. and Hungr, O. (eds) Debris-flow Hazards and Related Phenomena. Praxis, Heidelberg, Springer, Berlin, pp. 159–202.

Pierson, T.C. and Janda, R.J. 1994. Volcanic mixed avalanches: A distinct eruption-triggered mass flow process at snow-clad volcanoes Geological Society of America Bulletin, 106, 1351-1358.

Pierson, T.C. and Scott, K.M. 1985. Downstream dilution of a lahar: Transition from a debris flow to a hyperconcentrated streamflow. Water Resources Research, 21, 1511-1524.

Pierson, T.C., Janda, R.J., Thouret, J.-C. and Borrero, C.A. 1990. Perturbation and melting of snow and ice by the 13 November 1985 eruption of Nevado del Ruiz, Colombia, and consequent mobilization, flow and deposition of lahars. Journal of Volcanology and Geothermal Research, 41, 17-66.

Pierson, T.C. and Waitt, R.B. 1999a. Hydrologic consequences of hot-rock/snowpack interactions at Mount St. Helens volcano, Washington, 1982-84. Introduction. United States Geological Survey Professional Paper, 1586, 1-8.

Pierson, T.C. and Waitt, R.B. 1999b. Dome-collapse rockslide and multiple sediment-water flows generated by a small explosive eruption on February 2-3, 1983. United States Geological Survey Professional Paper, 1586, 53-68.

Pollock, M., Edwards, B.R., Hauksdottir, S., Alcorn, R. and Bowman, L. 2014. Geochemical and lithostratigraphic constraints on the formation of pillow-dominated tindars from Undirhlíðar quarry, Reykjanes Peninsula, southwest Iceland. Lithos, 200-201, 317-333.

Procter, J., Zernack, A., Mead, S., Morgan, M. and Cronin, S. 2021. A review of lahars; past deposits, historic events and present-day simulations from Mt. Ruapehu and Mt. Taranaki, New Zealand. New Zealand Journal of Geology and Geophysics, 64, 479-503.

Rignot, E., Mouginot, J. and Scheuchl, B. 2011. Ice flow of the Antarctic Ice Sheet. Science, 333, 1427-1430.

Roberts, M.J., Russell, A.J., Tweed, F.S. and Knudsen, Ó. 2000. Ice fracturing during jökulhlaups: implications for englacial floodwater routing and outlet development. Earth Surface Processes and Landforms, 25, 1429-1446.

Roberts, M.J. and Gudmundsson, M.T. 2015. Öræfajökull volcano: geology and historical floods. In: Pagneux, E., Gudmundsson, M.T., Karlsdóttir, S. and Roberts, M.J. (eds) Volcanogenic floods in Iceland. An assessment of hazards and risks at Öræfajökull and on the Markarfljót plain. Rekjavik: IMO, IES-UI, NCIP-DCPEM, pp. 17-43.

Russell, A.J. and Knudsen, Ó. 1999. An ice-contact rhythmite (turbidite) succession deposited during the November 1996 catastrophic outburst flood (Jökulhlaup), Skeiðarárjökull, Iceland. Sedimentary Geology, 127, 1-10.

Russell, A.J., Tweed, F.S. and Knudsen, Ó. 2000. Flash flood at Sólheimajökull heralds the reawakening of an Icelandic subglacial volcano. Geology Today, 16, 102-106.

Russell, A.J., Roberts, M.J., Fay, H., Marren, P.M., Cassidy, N.J., Tweed, F.S. and Harris, T. 2006. Icelandic jökulhlaup impacts: Implications for ice-sheet hydrology, sediment transfer and geomorphology. Geomorphology, 75, 33-64.

Russell, A.J., Duller, R. and Mountney, N.P. 2010a. Volcanogenic jökulhlaups (glacier outburst floods) from Mýrdalsjökull: impacts on proglacial environments. Developments in Quaternary Sciences, 13, 181-207.

Russell, A.J., Tweed, F.S., Roberts, M.J., Harris, T.D., Gudmundsson, M.T., Knudsen, Ó. and Marren, P.M. 2010b. An unusual jökulhlaup resulting from subglacial volcanism, Sólheimajökull, Iceland. Quaternary Science Reviews, 29, 1363-1381.

Russell, J.K., Edwards, B.R., Porritt, P. and Ryane, C. 2014. Tuyas: a descriptive genetic classification. Quaternary Science Reviews, 87, 70-81.

Russell, J.K., Edwards, B.R., Turnbull, M. and Porrit, L.A. 2021. Englacial lake dynamics within a Pleistocene cordilleran ice sheet at Kima' Kho (British Columbia, Canada). Quaternary Science Reviews, 273, 107247, doi.org/10.1016/j.quascirev.2021.10724

Schopka, H.H., Gudmundsson, M.T. and Tuffen, H 2006. The formation of Helgafell, southwest Iceland, a monogenetic subglacial hyaloclastite ridge: Sedimentology, hydrology and volcano-ice interaction. Bulletin of Volcanology, 152, 359-377.

Scott, K.M. 1988. Origins, behavior, and sedimentology of lahars and lahar-runout flows in the Toutle-Cowlitz river system, Mount St. Helens, Washington. United States Geological Survey Professional Paper, 1447-A, 1-76.

Scott, K.M., Vallance, J,W. and Pringle, P.T. 1995. Sedimentology, behavior, and hazards of debris flows at Mount Rainier, Washington. United States Geological Survey Professional Paper, 1547, 1-56.

Sigvaldason, G.E. 1992. Recent hydrothermal explosion craters in an old hyaloclastite flow, central Iceland. Journal of Volcanology and Geothermal Research, 54, 53-63.

Simpson, K.A., Stasiuk, M., Shimamura, K., Clague, J.J. and Friele, P. 2006. Evidence for catastrophic volcanic debris flows in Pemberton Valley, British Columbia. Canadian Journal of Earth Sciences, 43, 679-689.

Skilling, I.P. 1994. Evolution of an englacial volcano: Brown Bluff, Antarctica. Bulletin of Volcanology, 56, 573-591.

Smellie, J.L. 2001. Lithofacies architecture and construction of volcanoes in englacial lakes: Icefall Nunatak, Mount Murphy, eastern Marie Byrd Land, Antarctica. In: White, J.D.L. and Riggs, N. (eds) Lacustrine volcaniclastic sedimentation. IAS Special Publication, 30, pp. 73-98.

Smellie, J.L. 2002. The 1969 subglacial eruption on Deception Island (Antarctica): events and processes during an eruption beneath a thin glacier and implications for volcanic hazards. Geological Society, London, Special Publication, 202, 59-79.

Smellie, J.L. 2006. The relative importance of supraglacial versus subglacial meltwater escape in basaltic subglacial tuya eruptions: An important unresolved conundrum. Earth-Science Reviews, 74, 241-268.

Smellie, J.L. 2008. Basaltic subglacial sheet-like sequences: Evidence for two types with different implications for the inferred thickness of associated ice. Earth-Science Reviews, 88, 60-88.

Smellie, J.L. 2009. Terrestrial sub-ice volcanism: landform morphology, sequence characteristics and environmental influences, and implications for candidate Mars examples. Geological Society of America Special Papers, 453, 55-76.

Smellie J.L. 2013. Quaternary vulcanism: subglacial landforms. In: Elias S.A. (ed.) The encyclopedia of Quaternary science, 2nd edition, Vol. 1, Elsevier, Amsterdam, pp. 780-802.

Smellie, J.L. 2018. Glaciovolcanism – a 21st century proxy for palaeo-ice. In: Menzies, J. and van der Meer, J.J.M. (eds) Past Glacial Environments (sediments, forms and techniques), 2nd edition. Elsevier, Amsterdam, Netherlands, pp. 335-375.

Smellie, J.L., Hole, M.J. and Nell, P.A.R. 1993. Late Miocene valley-confined subglacial volcanism in northern Alexander Island, Antarctic Peninsula. Bulletin of Volcanology, 55, 273–288.

Smellie J.L. and Skilling, I.P. 1994. Products of subglacial eruptions under different ice thicknesses: two examples from Antarctica. Sedimentary Geology, 91, 115-129.

Smellie J.L., Rocchi, S. and Armienti, P. 2011a. Late Miocene volcanic sequences in northern Victoria Land, Antarctica: products of glaciovolcanic eruptions under different thermal regimes. Bulletin of Volcanology, 73, 1-25.

Smellie J.L., Rocchi, S., Gemelli, M., Di Vincenzo, G. and Armienti, P. 2011b. Late Miocene East Antarctic ice sheet characteristics deduced from terrestrial glaciovolcanic sequences in northern Victoria Land, Antarctica. Palaeogeography, Palaeoclimatology, Palaeoecology, 307, 129-149.

Smellie, J.L. and Edwards, B.R. 2016. Glaciovolcanism on Earth and Mars. Products, processes and palaeoenvironmental significance. Cambridge University Press, Cambridge, 483 pp.

Smellie, J.L., Walker, A.J., McGarvie, D.W. and Burgess, R. 2016. Complex circular subsidence structures in tephra deposited on large blocks of ice: Varða tuff cone, Öræfajökull, Iceland. Bulletin of Volcanology, 78, 56, doi:10.1007/s00445-016-1048-x

Smellie, J.L. Rocchi, S., Johnson, J.S., Di Vincenzo, G. and Schaefer, J.M. 2018. A tuff cone erupted under frozen-bed ice (northern Victoria Land, Antarctica): linking glaciovolcanic and cosmogenic nuclide data for ice sheet reconstructions. Bulletin of Volcanology, 80, 12, doi:10.1007/s00445-017-1185-x

Smellie, J.L. and Panter, K.S. 2021. Lithofacies and eruptive conditions of the southernmost volcanoes in the world (87° S). Bulletin of Volcanology, 83, 49, doi.org/10.1007/s00445-021-01475-y

Stefánsdottir, M.B. and Gíslason, S.R. 2005. The erosion and suspended matter/seawater interaction during and after the 1996 outburst flood from the Vatnajökull Glacier, Iceland. Earth and Planetary Science Letters, 237, 433-452.

Stevenson, J.A., McGarvie, D.W., Smellie, J.L. and Gilbert, J.S. 2006. Subglacial and ice-contact volcanism at Vatnafjall, Öraefajökull, Iceland. Bulletin of Volcanology, 68, 737-752.

Stevenson, J.A., Smellie, J.L., McGarvie, D.W. and Gilbert, J.S. 2009. Subglacial intermediate volcanism at Kerlingarfjöll, Iceland: magma-water interactions beneath thick ice. Journal of Volcanology and Geothermal Research, 185, 337-351.

Stevenson, J.A., Gilbert, J.S., McGarvie, D.W. and Smellie, J.L. 2011. Explosive rhyolite tuya formation: classic examples from Kerlingarfjöll, Iceland. Quaternary Science Reviews, 30, 192-209.

Sturm, M., Beget, J. and Benson, C. 1987. Observations of jökulhlaups from ice-dammed Strandline Lake, Alaska: implications for paleohydrology. In: Mayer, L. and Nash, D. (eds) Catastrophic flooding. Allen and Unwin, pp. 79-94.

Thouret, J.-C. 1990. Effects of the November 13, 1985 eruption on the snow pack and ice cap of Nevado del Ruiz volcano, Colombia. Journal of Volcanology and Geothermal Research, 41, 177–201.

Thouret, J.-C., Salinas, R. and Murcia, A. 1990. Eruption and mass-wasting-induced processes during the late Holocene destructive phase of Nevado del Ruiz volcano, Colombia. Journal of Volcanology and Geothermal Research, 41, 203-224.

Thouret, J.-C., Antoine, S., Magill, C. and Ollier, C. 2020. Lahars and debris flows: Characteristics and impacts. Earth-Science Reviews, 201, 103003, doi.org/10.1016/j.earscirev.2019.103003

Tómasson, H. 1975. Grímsvatnahlaup 1972, mechanism and sediment discharge. Jökull, 24, 27–39.

Tómasson H. 1996. The jökulhlaup from Katla in 1918. Annals of Glaciology, 22, 249–254.

Trabant, D.C., Waitt, R.B. and Major, J.J. 1994. Disruption of Drift glacier and origin of floods during the 1989-1990 eruptions of Redoubt Volcano, Alaska. Journal of Volcanology and Geothermal Research, 62, 369-385.

Tuffen, H., Gilbert, J. and McGarvie, D. 2001. Products of an effusive subglacial rhyolite eruption: Bláhnúkur, Torfajökull, Iceland. Bulletin of Volcanology, 63, 179-190.

Tuffen, H., McGarvie, D.W., Gilbert, J.S. and Pinkerton, H. 2002. Physical volcanology of a subglacial-to-emergent rhyolitic tuya at Raudufossafjöll, Torfajökull, Iceland. Geological Society, London, Special Publications, 202, 213-236.

Tweed, F.S. and Russell, A.J. 1999. Controls on the formation and sudden drainage of glacier-impounded lakes: implications for 49ökulhlaups characteristics. Progress in Physical Geography, 23, 79-110.

Vallance, J.W. and Scott, K.M. 1995. The Osceola Mudflow from Mount Rainier: Sedimentology and hazard implications of a huge clay-rich debris flow. Geological Society of America Bulletin, 109, 143-163.

Vallance, J.W. and Iverson, R.M. 2015. Lahars and their deposits. In: Sigurdsson, H., Houghton, B., Rymer, H., Stix, J. and McNutt, S. (eds) The Encyclopedia of Volcanoes, 2nd Edition. Academic Press, San Diego, pp. 649-664.

van der Bilt, W.G.M., Barr, I.D., Berben, S.M.P., Hennekam, R., Lane, T., Adamson, K. and Bakke, J. 2021. Late Holocene canyon-carving floods in northern Iceland were smaller than previously reported. Communications, Earth & Environment, 2, 86, doi.org/10.1038/s43247-021-00152-4

Waitt, R.B., 1989. Swift snowmelt and floods (lahars) caused by great pyroclastic surge at Mount St. Helens volcano, Washington, 18 May 1980. Bulletin of Volcanology, 52, 138-157.

Waitt, R.B. 1995. Hybrid wet flows formed by hot pyroclasts interacting with snow during the 1992 eruptions of Crater Peak, Mount Spurr volcano, Alaska. United States Geological Survey Bulletin, 2139, 107-118.

Waitt, R. B., Pierson, T.C., MacLeod, N.S., Janda, R.J., Voight, B. and Holcomb, R.T. 1983. Eruption-triggered avalanche, flood, and lahar at Mount St. Helens—Effects of winter snowpack. Science, 221, 1394-1397.

Waitt, R.B., Gardner, C.A., Pierson, T.C., Major, J.J. and Neal, C.A. 1994. Unusual ice diamicts emplaced during the December 15, 1989 eruption of Redoubt Volcano, Alaska. Journal of Volcanology and Geothermal Research, 62, 409-428.

Walder, J.S. 1999. Nature of depositional contacts between pyroclastic deposits and snow or ice. United States Geological Survey Professional Papers, 1586, 9-18.

Walker, G.P.L. and Blake, D.H. 1966. The formation of a palagonite breccia mass beneath a valley glacier in Iceland. Journal of the Geological Society, London, 122, 45–61.

Waller, R.J., Russell, A.J., van Dijk, T.A.G.P. and Knudsen, Ó. 2001. Jökulhlaup-related ice fracture and supraglacial water release during the November 1996 jökulhlaup, Skeiðarárjökull, Iceland. Geografiska Annaler, 83A, 29-38.

Waythomas, C.F., Pierson, T.C., Major, J.J. and Scott, W.E. 2009. Voluminous ice-rich and water-rich lahars generated during the 2009 eruption of Redoubt Volcano, Alaska. Journal of Volcanology and Geothermal Research, 259, 389-413.

Werner, R. and Schmincke, H.-U. 1999. Englacial vs lacustrine origin of volcanic table mountains: evidence from Iceland. Bulletin of Volcanology 60, 335–354.

White, J.D.L., Smellie, J.L. and Clague, D.A. (eds) 2003. Explosive subaqueous volcanism. American Geophysical Union, Geophysical Monograph, 140, 379 pp.

White, J.D.L. and Houghton, B.F. 2006. Primary volcaniclastic rocks. Geology, 34, 677-680.

Wilson, L., Smellie, J.L. and Head, J.W. 2013. Volcano—ice interactions. In: Fagents, S.A., Gregg, T.K.P. and Rosaly, M.C. (eds) Modeling volcanic processes: the physics and mathematics of volcanism. Cambridge University Press, Cambridge, UK, pp. 275-299.

Zimanowski, B. and Büttner, R. 2003. Phreatomagmatic explosions in subaqueous volcanism. In: White, J.D.L., Smellie, J.L. and Clague, D.A. (eds) Explosive subaqueous volcanism. American Geophysical Union, Geophysical Monograph 140, pp. 51-60.